Large power transformers: time now for addressing their monitoring and failure investigation techniques

Jonathan Velasco Costa [1,‡] **Diogo F. F. da Silva** [2,‡] **and P. J. da Costa Branco** [3,*]

IDMEC, Instituto Superior Técnico, Universidade de Lisboa

1   jonathanvelasco@tecnico.ulisboa.pt
2   diogo.da.silva@tecnico.ulisboa.pt
3   pbranco@tecnico.ulisboa.pt
*   Corresponding author
‡   These authors contributed equally to this work.

Abstract: Large power transformers are generally associated with a maximum capacity rating of 100 MVA or higher. These large liquid dielectric power transformers are a custom-built piece of equipment, thus very expensive, and a backbone element of the power grid. In extreme cases as, for example, severe geomagnetic disturbances, permanently monitoring their condition will enhance their electrical reliability and resilience to guarantee efficient management of its life cycle. However, some traditional monitoring/diagnosis techniques have singular features when applied to large power transformers and their interlinked subsystems. In this context, and since that information is hardly put in evidence and compiled in the literature, this paper reviews the particularities of monitoring and diagnosing those assets.

Keywords: Large power transformer; condition monitoring; transformer fault diagnosis; diagnostic techniques; mechanical or electrical integrity of the core and windings

1. Introduction

Large power transformers (LPT) are custom-built pieces of equipment that are crucial links to the bulk transmission grid. Usually, they link a generator-transmission line and/or linking lines of different voltages. LPTs are characterized by technical and logistic features, making them a special case for condition monitoring of power transformers. These features are:

1. LPTs are usually neither interchangeable nor produced for extensive spare inventories since they are very expensive and tailored to customers' specifications. LPTs can cost millions of euros, and each device weights between approximately 100 and 400 tons [1];

2. Replacing an LPT after a failure can be difficult because of the limited availability of spare devices. This is a potential issue about the required resilience of the power grid [2,3];

3. Unfortunately, being a piece of custom-built equipment, the production process of LPTs can extend beyond 20 months if, for example, the manufacturer has difficulty obtaining certain key parts or materials for LPT's production (ex: acquisition of special grade electrical steel);

4. The average age of installed LPTs in the United States and Europe is over 20 years [4]. While the life expectancy of a power transformer varies depending on how and

where it is used, aging power transformers are potentially subject to an increased risk of failure. Figure 1 shows how age is certainly a contributing factor to increase the transformer failures rate when installed in industrial plants, generation plants, and transmission networks. The failure rate curves are sharper for industrial and generator transformers because the transformers in these installations tend to be exploited more intensively.
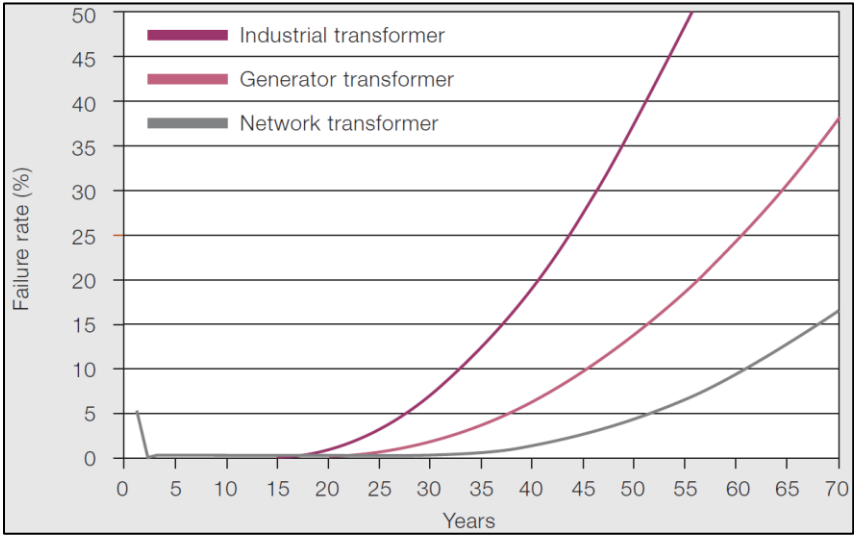

Figure 1 – Aging contributes to increasing the LPTs failures rate when installed in industrial plants, generation plants, and transmission networks [5].
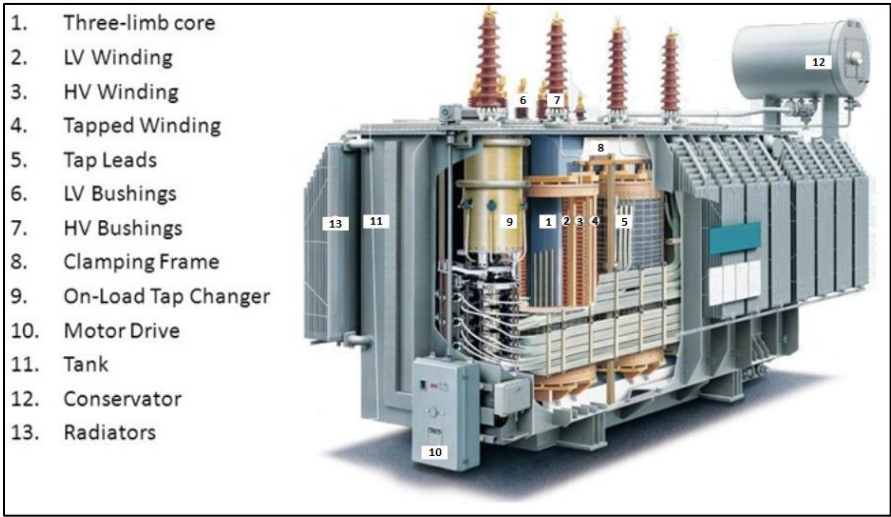

Figure 2 – Standard core-type large power transformer and its major internal components.

According to [6], LPTs are in general divided into transmission transformers, with the low voltage side rated 100 kV or higher and the maximum nameplate rating 100 MVA or higher; and generation stet-up transformers, with high voltage side rated 100 kV or higher and the maximum nameplate rating 75 MVA or higher. Figure 2 illustrates a standard core-type LPT and its major internal components.

The LPT key characteristics can be summarized as large, tailored to certain customer specifications, expensive, rarely interchangeable, or produced for extensive spare inventories. To understand how LPTs can differ in some aspects, a localized power outage at the distribution level (distribution transformers) will not present significant reliability threats, and utilities often maintain spare transformer equipment of their size range. An outage of an LPT is completely out of this reality. Figure 2 illustrates a standard core-type LPT and its major internal parts and components: the core, which is made of high-permeability, grain-oriented, silicon electrical steel laminations; the electrical input-output windings, which are made of copper conductors wound around the core; the tank where core and windings are contained; the bushings connecting the LPT to transmission line; the tap-changer, power cable connectors, gas-operated relays, thermometers, relief devices, dehydrating breathers, oil level indicators, and other controls.

In this context, it is more than justified for LPTs to detect and identify failures at their early stage to implement preventive actions, which is achieved mainly through continuous monitoring of the transformer. In addition, if the LPT condition of this equipment is continuously monitored in time, it is possible to manage its life cycle. In other words, it will be possible to define maintenance actions based on the condition of this critical asset rather than providing preventive maintenance, which is nowadays the common practice and is carried out at specific time intervals.

The present paper summarizes large power transformers' particularities of monitoring and diagnosis for these assets. Unlike other similar reviews, this will mirror the authors' experience with a 1400 MVA phase-shift LPT in service since 2007 manufactured by ABB with a nominal voltage on the primary and secondary side of 400 kV phase-shifting within ±25°.

2. Oil-immersed large power transformers: abnormal operating conditions

In the current context of deregulation of electricity systems and mainly under the conditions mentioned in the introduction, each electricity company seeks to manage its assets more efficiently, basing itself on conditional and proactive maintenance methodologies. This pursues to limit the number of interruptions in the grid and thus avoid economic penalties that can be severe. More specifically, only one large power transformer's shutdown can lead to direct and indirect losses that would far exceed its price [7].

It is even more essential for large power transformers to understand which condition of their components indicates an *abnormal operation*. To systematize this point, it is shown in Figure 3 a drawing cut of a typical large power transformer and its main components. The potential and associated abnormal conditions are presented based on those identified.
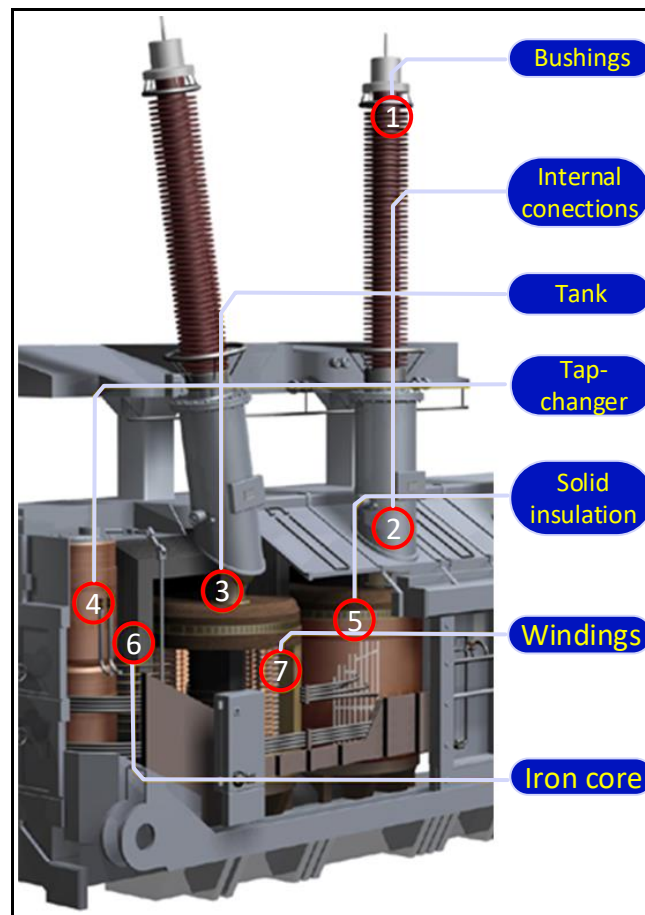
Figure 3 – A large power transformer and its main components.

2.1   Active Part

2.1.1   Windings

The windings' abnormal operating conditions are one of the most frequent causes of failures, for they can experience wear at the mechanical, thermal, and dielectric levels [8]. These three always appear in a coupled way, and, most often, one of the phenomena proves to be more significant for the appearance of failure.

Mechanical anomalies are the loosening, displacement, or deformation of the windings [9,10], as shown in Figure 4 left. These anomalies originate from improper repair, poor maintenance, corrosion, manufacturing defects, vibrations, and mechanical displacements within the transformer. On the other side, windings can present high thermal losses in events such as a short circuit in the outer terminals. These losses usually give rise to "hot spots" that can lead to small ruptures or even the total copper breaking in the windings.

Dielectric anomalies come from disruptions of the insulating material between phases. Disruption occurs due to high potential differences such that the resulting electric field causes ruptures within the dielectric material. These can occur between turns of the same phase or between phases. Often, disruption will result in the appearance of small short circuits that will lead to local burning of the windings [11], as shown in Figure 4 right.
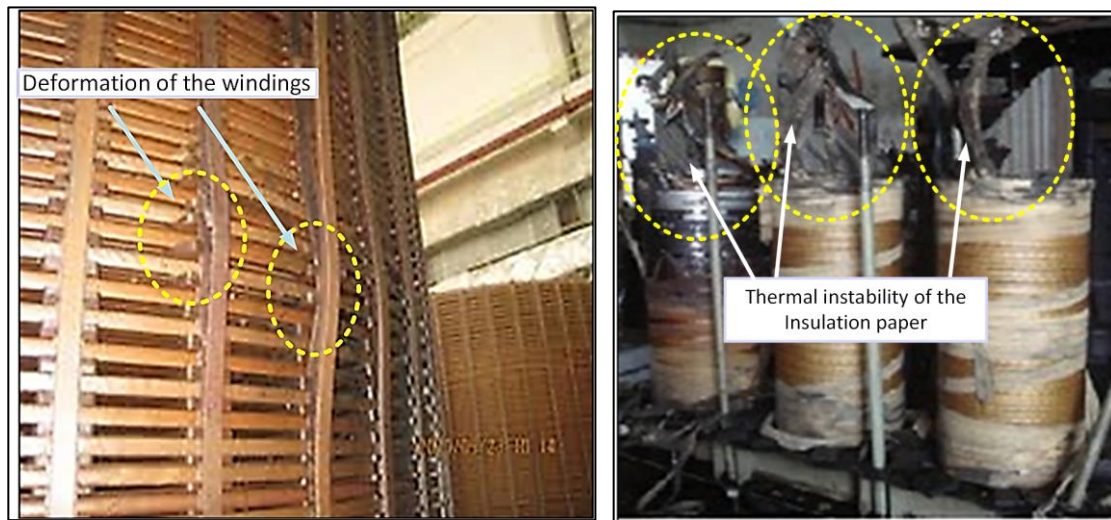
Figure 4 – Examples of abnormal conditions in the windings, at left figure [9], there is a deformation of the windings. In the right figure [10], there is a dielectric failure (poor condition of the insulation paper).

2.1.2 Transformer core

One of the most frequent defects in the core [12] is shown in Figure 5. The displacement of the core blades due to electromagnetic forces is verified due to high eddy currents that circulated in them. In this situation, each conductor (blade) with an induced current produces a magnetic field that, when interacting with the currents circulating in the opposite blade, provokes electromagnetic forces in it, which causes a deformation in the plates [13]. Figure 6 shows an illustration of this phenomenon. If the laminations presented induced currents circulating in opposite directions, this would cause the appearance of repulsive electromagnetic forces, as occurred in Figure 5, otherwise appear attractive forces between laminated sheets.
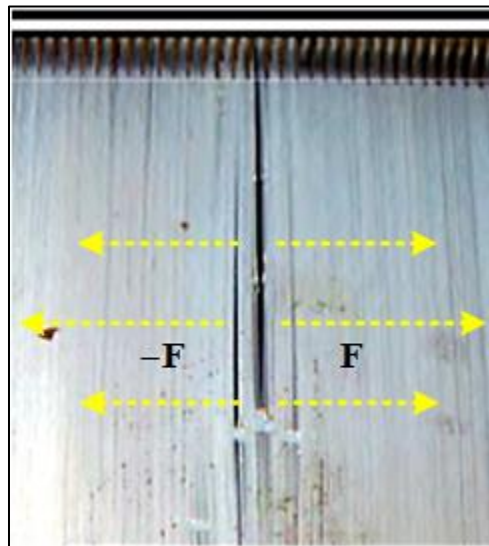

Figure 5 – Illustration of a power transformer case presenting mechanical deformation of the core and laminated electrical sheets [12].
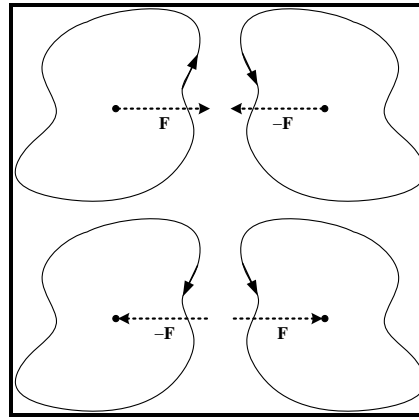
Figure 6 - Illustration of forces according to the current direction.

2.2   Insulation system

2.2.1   Solid insulation

Solid insulation is based on cellulose, namely paper and pressed wooden impregnated with oil forming a dielectric and mechanical insulation of the windings. The abnormal operating conditions that arise in these elements result mainly from the degradation of cellulose. The degradation has three mechanisms as its basis: hydrolysis (decomposition of the chemical compound by reaction with water), pyrolysis (decomposition or transformation of the compound by the action of heat), and oxygenation (combination of a substance with oxygen) [14]. The hydrolysis phenomenon is the mechanism that contributes most to the breakdown of the long chains of glucose rings that make up cellulose. This degradation and aging of cellulose significantly contribute to the loss of dielectric and mechanical properties that lead, for example, to short circuits between windings.

2.2.2   Liquid insulation

The dielectric fluid has two objectives: insulating the transformer core and its tank and cooling the transformer by convection. The oil circulates through the main tank, absorbed by the paper (helps its cooling), giving it special dielectric characteristics. Oil circulation also allows the removal of heat to the environment, as the oil, when heating, rises and enters the pipe that leads to the radiator.

The quality of the used oil greatly affects the properties of the insulation and cooling systems as particles (water, rust, and acids) appear in it due to its aging [15,16]. These make the oil more viscous, making its circulation difficult, thus putting the transformer's cooling capacity at risk. If these particles are electrical conductors, such as water, they can facilitate short-circuits between elements, representing a failure of the insulation system.

2.3   Components and accessories

2.2.1   Bushings

Another type of transformer anomaly occurs in their bushings (Figure 7), which serve as insulation between the passage of the outer conductors and the interior connection to the windings; they act as a path for the current of each stage to go through the walls of the tank.

The bushings can be of the capacitive or non-capacitive type, and for transformers, with higher operating voltages, it is usual to use the capacitive type bushings (Figure 6). Capacitive type bushings are classified as "OIP" (Oil Impregnated Paper - layers of oil-impregnated paper), "RIP" (Resin Impregnated Paper - paper impregnated with epoxy resins), and "RBP" (Resin Bonded Paper - layers of Bakelitized paper), the manufacture

of the latter being practically abandoned due to problems related to partial discharges [17].
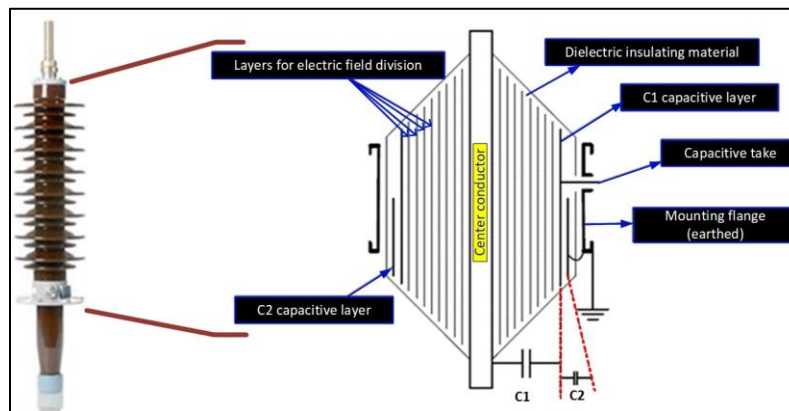

Figure 7 – OIP bushing and capacitive bushings scheme.

In Figure 7 left, it is possible to visualize an OIP bushing, and in Figure 7 right, it represents its scheme. The bushing is composed of a central conductor covered with paper impregnated in oil or resin (considering only the bushings of the OIP and RIP type) and the external insulator, usually in porcelain. The bushing is represented by a center conductor and several condensers between this and the mounting flange, as represented from its diagram in (Figure 7 right). Between the central conductor and the capacitive tap (where measurements are taken), there is the capacitor C1, which represents the value of the total capacitance in series resulting from the different layers of electric potential distribution. The capacitor C2 translates the capacitance value between the capacitive layer C2 and the capacitive tap; it corresponds to the insulation between C1 and the mounting flange [18].

Degradation of bushings, mainly those located at the high-voltage side, is essentially reflected in the appearance of partial discharges and the loss of dielectric properties that will lead to their overheating, as illustrated in Figure 8. This degradation may be due to the following set of factors:

1. Contamination of insulators, due to deposition of contaminants (water, dust) on the surface of bushings [19], and for highly polluted places they must be washed regularly;
2. Water ingress, which can enter, for example, through small cracks in the porcelain, which can be the result of mechanical damage to the bushing or else due to the bushing swelling and deflating with temperature [20];
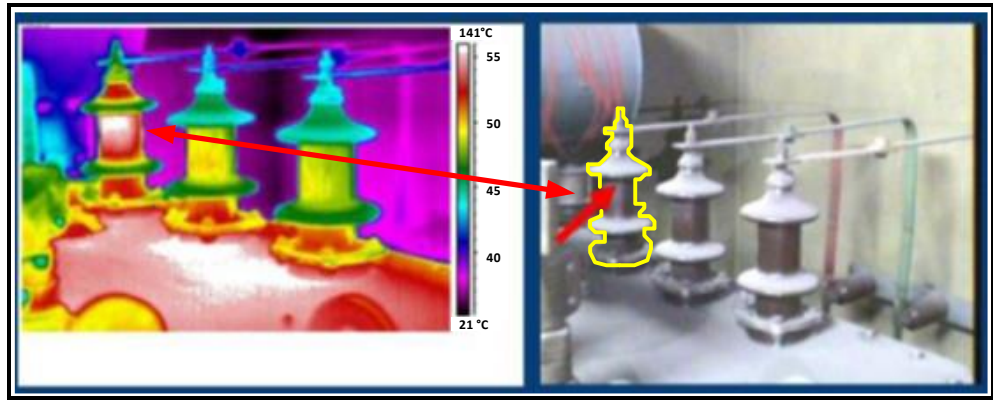3. Aging process of the bushing [21, 22].
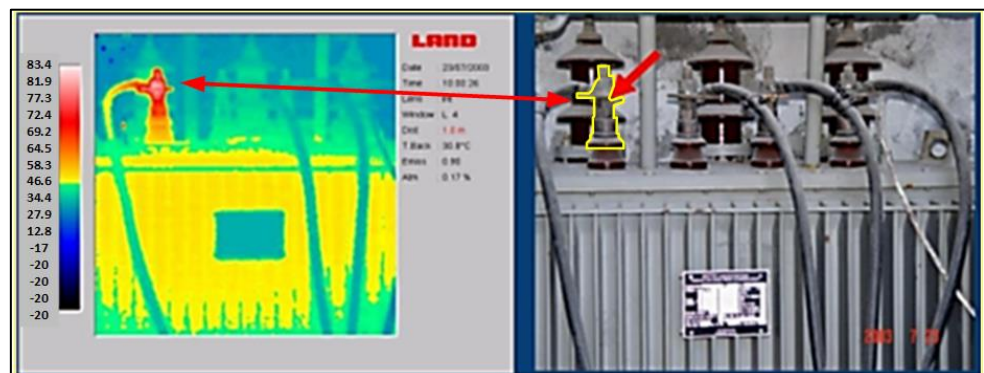
Figure 8 – Thermographic photographs of overheating bushings [23].

2.2.1   Tap-changer

Tap-changer is one of the most critical components of a large power transformer [24] as it is one of the only that exhibits a controlled displacement (Figure 9 left). It can regulate the voltage and/or phase change by varying the ratio of the number of turns of the transformer without interrupting the load, thus allowing for the compensation of constant load variations. There are essentially two types of tap-changers: those using resistors or reactances during the switching process. The first is usually installed inside the tank (they can have their oil or share the oil), while the second is usually welded to the tank [25]. In Europe, in particular, it is usual to use resistive-type tap-changers.

The tap-changer is composed of a "switch" switching component and a "plug selector" selection component, as illustrated in Figure 9 right. The entire switching process is driven by a single-phase induction motor placed outside the transformer.

Variation of the number of turns ratio is intended to be carried out without interrupting the load current. The process always occurs by connecting the next socket before undoing the previous connection. To avoid the high current coming from the short circuit between turns, a transition impedance is inserted in the form of electrical resistance or reactance, thus achieving the transfer of the load current from one socket to the other.
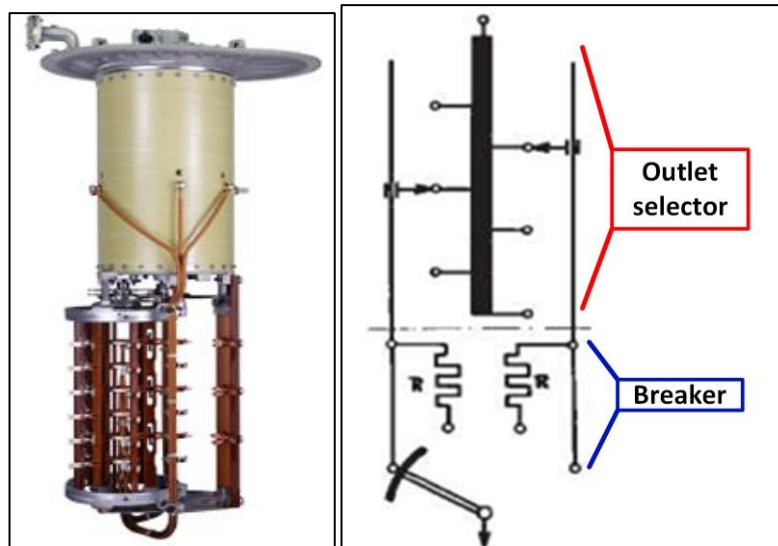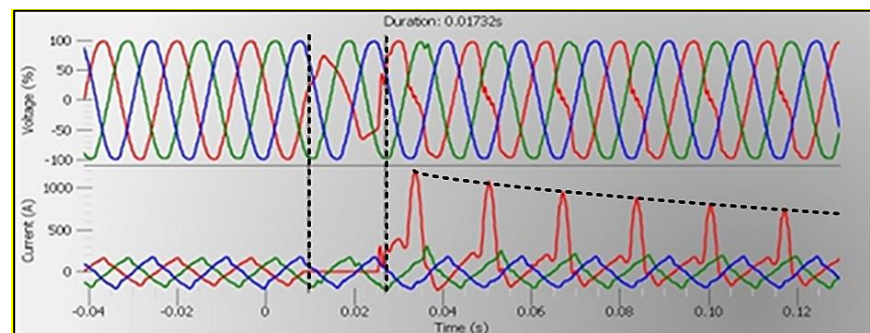

Figure 9 - On-load tap-changer [19].

In the on-load voltage regulator, abnormal operating conditions may also arise, which will be reflected in the operation of the transformer. Some of them are presented below.

1. The lack of maintenance of this equipment can lead to a desynchronization between the selector and the tap-changer, causing the voltage regulator not to be in the correct position [26,27];
2. Old or burnt condensers in the induction motor can lead to a loss of control in the direction of governor movement or even cause the governor motor to stop and make it impossible to change the number of turns ratio;
3. With frequent use, commutator springs lose elasticity and may even break. In this case, it will not be possible to change the ratio of number of turns of regulator [28];
4. The voltage regulator is frequently used, which leads to wear of the entire switching mechanism [29], especially in the contacts responsible for the transition of plugs, which are subject to electric arcs. In the on-load voltage regulator, the interruption of current leads to the appearance of an electric arc, which leads to the formation of gases that are the same as those that appear in the main transformer tank due to dielectric failures. As such, if the tank is shared, false conclusions about dielectric failures and their location can result;
5. When operating on the same contact for a long time, there is a risk of deposition of carbon particles, which can char due to the heat from the increased contact resistance. In extreme cases, as shown in Figure 10(a), the contacts' carbonization leads to the impossibility of operation as the contacts are stuck [30]. This anomaly is not very common in on-load voltage regulators, being more relevant for no-load voltage regulators.

The example illustrated in Figure 10(a) occurred in a substation transformer and showed the occurrence of a severe failure in the regulator switch. As can be seen from the evolution of voltages and currents at the transformer terminals in Figure 10(b), the fault was reflected in the signals by the appearance of oscillations in one of the currents and the deformation associated with the respective voltage.

(a)

(b)

Figure 10 - Abnormal condition in the on-load tap-changer (a) and current and voltage signals at the transformer terminals (b) [30].

2.2.1 Tank

The tank contains the oil and provides physical protection and support for the different components of the transformer, besides ensuring the grounding of the magnetic circuit and the various metal parts. The tank may show cracks [31], essentially resulting from environmental wear and tear, such as those resulting from corrosive environments, high humidity, vibrations, and solar radiation. The tank walls may also be subject to rupture due to high-pressure gases resulting from internal arcs that vaporize the oil [32].

2.2.2 Cooling system

In a large power transformer, cooling is achieved through the forced circulation of oil and water or air. Forced circulation is based on the use of pumps and fans. There is a coding depending on the internal and external cooling medium and the type of circulation they are subject to. For example, ONAN is interpreted as having internal cooling medium mineral oil and external air, and the circulation in both is characterized by being natural. Generally, internal cooling uses mineral oil "O" forced through the radiators and directed from these to the "D" windings, or even if it is just forced "F." External cooling uses "A" air or "W" water. For external circulation, there is "N" for natural air convection and "F" for forced circulation. The same transformer can have several types of cooling, that is, depending on the temperature and/or power to which it is subject, it can activate or deactivate the fans and/or pumps [33, 34].

The most significant anomalies in the cooling system lead to an increase in the temperature of the transformer oil, which affects different components of the transformer and can even lead to an increase in the pressure of the gases that form, leading to its explosion [35]. These failures can, for example, originate from cracks in the tubes where the oil circulates (causes a reduction in the amount of oil and leading to a reduction in heat exchange), or even due to anomalies in the fans due to wrong measurements of the thermometers or malfunction of the ventilation and pumping system. The example from [36] in Figure 11 makes it possible to visualize a case in which the oil level dropped and prevented its circulation since the radiator valves are at a lower level.
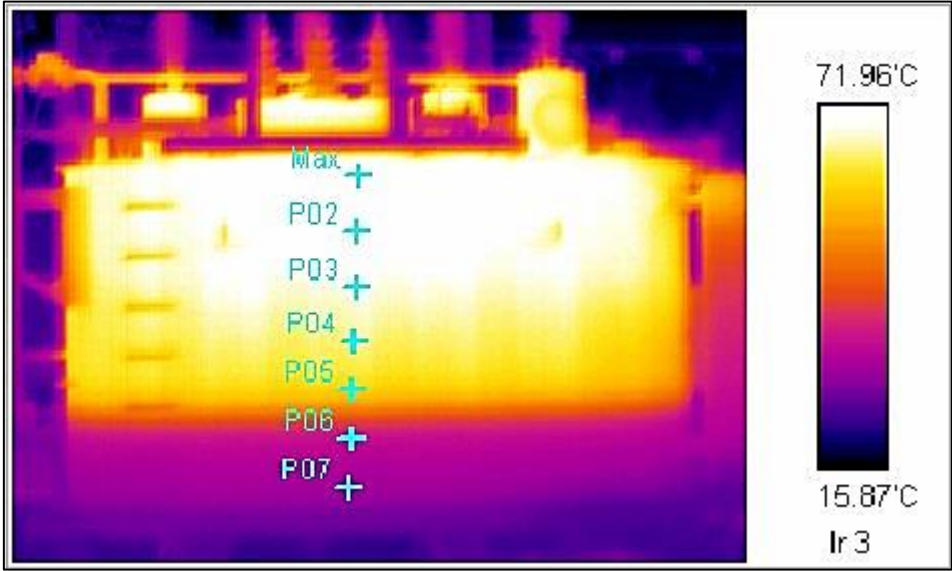
Figure 11 - Transformer thermographic photograph [36].

Until now, we pointed out various abnormal operating conditions that lead to transformer failure. However, it is not straightforward to enumerate them all. Hence, we decided to outline the most frequent anomalies associated with each transformer system element. Table 1 summarizes, based on the information presented above and in [37, 38], the failure modes and most recurrent causes that appear in each component.

Table 1. Failure modes and common causes are associated with the most important transformers' components.

Component	Failure Mode	Event	Cause
Core	Loss of efficiency	Blade displacement	- Eddy currents
Windings	Short-circuit	Mechanical damage	- Manufacturing deficiencies - Corrosion - Bad maintenance - Vibrations - Mechanical displacements
		Insulation Failure	- Overvoltage - Overheating
Solid insulation	Cannot provide insulation	Mechanical damage	- Cellulose aging
		Insulation Failure	- Cellulose Aging - Overheating
Insulation fluids	Short-circuit	Conductive particles in the oil	- Aging - Overheating
	Overheating	Oil does not cool	- Pumps/Fans failure - Particles in oil (aging and overheating)
Bushings	Overheating	Partial discharges and loss of dielectric properties	- Insulator contamination - Water inlet - Aging
On-load voltage regulator	Inability to change the number of turns ratio	Mechanical damage	- Breakage of springs - Lack of maintenance - Old or burnt condensers - Carbonization - Switching system wear
Oil tank	Oil leakage	Damage to tank walls	- High gas pressure - Environmental wear
Cooling system	Overheating	Cooling incapacity	- Pipe cracks - Particles in oil (aging and overheating) - Pump/fan failures

3. Traditional diagnostic methods

A faulty transformer can lead to situations that are sometimes significant in terms of their financial, technical, and environmental consequences. Hence, the need to detect and identify the fault as soon as possible.

As the price of a large power transformer is very high, simple oil analysis can be enough to avoid costly damage associated with a prolonged interruption of its operation. Hence, it will be preferable to follow the evolution and trends deduced from the information inferred from the analysis carried out on the oil.

The analysis of gases dissolved in oil by itself is quite incomplete. Faults pointed out by the various existing methods can have different origins, giving rise to different failures. Based on [39, 40, 41], Table 2 summarizes at a macro level the four major types of failures detected by analyzing the gases dissolved in the oil and potential reasons for them. However, to determine the source of a failure with accuracy, it is essential to

complement the analysis of gases dissolved in oil with other existing diagnostic methods, as discussed later.

Table 2. Major failures in large power transformers with signature detected by analyzing the gases dissolved in the oil [39, 40, 41].

Cause	Failure			
	High energy electrical discharge	Low energy electrical discharge	Paper overheating	Oil overheating
Short circuit between turns of the windings	X		X	
Winding open circuit	X		X	
Internal LTC Operation	X			
Deformation or displacement of windings		X	X	
Loss of connection of the crossing terminals	X	X	X	
Water or too much moisture in the oil	X	X		
Metallic particles in the oil	X	X		
Displacement of spacers		X		
Overload			X	
Insulation between blades damaged				X
Rust or other core damage				X
Obstacles to the passage of oil				X
Cooling system malfunction				X

3.1 *Dissolved gas-in-oil analysis*

Transformer diagnosis through an analysis of gases dissolved in oil, which fits into the philosophy of conditional maintenance, is a very effective preventive monitoring tool. It allows predicting the status and initial defects that may appear during transformer operation. As such, it is an essential technique in determining the transformer's "health status."

The two main causes of the formation of those gases are *electrical disturbances* and *thermal decomposition*. The rate at which each gas is produced depends essentially on the temperature and the volume of material. Transformer failure diagnosis has 8 key gases: hydrogen (H_2), methane (CH_4), ethane (C_2H_6), ethylene (C_2H_4), acetylene (C_2H_2), carbon monoxide (CO), and carbon dioxide (CO_2).

Failures detected by analyzing those gases are thermal failures, electrical discharges (low and high energy), and partial discharges. Thermal failures result from an excessive rise in insulation temperature and can occur in paper or oil. Thermal failures in oil are divided into several classes since, depending on the temperature, the gases formed differ. Here, terms as *low-* or *high-energy electrical discharges* refer to insulation disruptions between conductors [42, 43].

In Table 3, we present a color scale representing the association between the concentration rate of each gas and each type of failure occurring in the transformer. The table presented was constructed based on information collected from references [44-46]. The colors symbolize the different quantities of gases produced, with green being associated with small quantities (trace), yellow with medium quantities, and red with large quantities.

Table 3. Standardization regarding gases produced in the transformer and associated failures.

Failure	H_2	CH_4	C_2H_6	C_2H_4	C_2H_2	CO	CO_2
Thermal paper						(red)	(red)
Thermal oil [150-300°C]	(yellow)	(red)	(red)	(green)			
Thermal oil [300-700°C]	(red)	(yellow)	(yellow)	(yellow)	(green)		
Thermal oil [>700°C]	(red)	(yellow)	(green)	(red)	(yellow)		
Low energy discharge	(red)	(red)	(yellow)	(yellow)			
High energy discharge (Arc-electric)	(red)	(yellow)		(yellow)	(red)		
Partial discharge	(red)	(yellow)	(green)	(green)			

The total concentrations of the gases, their relative proportions, and the rate of increase of each gas makes it possible to assess the condition of the transformer. Several criteria allow associating these parameters with the type of failure that occurred, the most common currently being the method of Rogers [46], Doernenburg [47], IEC 60599 [47], Duval [48], Key Gas[48], and TDCG [49]. These criteria are empirical, and the results are based on the correlation between the detected gases. Many of them use ratios to determine the failure, which makes it possible to eliminate the oil volume effect and some sampling effects [50]. Below are some of the most used ratios and possible types of failure associated with [49,50]. Note that these are only significant and should only be calculated if at least one of the gases exceeds its typical concentration and growth rate value.

R1: (CH_4/H_2) - Partial Discharges
R2: (C_2H_2/C_2H_4) - Arc-electric
R3: (C_2H_2/C_2H_4)
R4: (C_2H_6/C_2H_2) - High intensity discharge
R5: (C_2H_4/C_2H_6) - Oil overheating > 500 °C
R6: (CO_2/CO) - Cellulose overheating
R7: $(N_2/O2)$ – Oxygen consumption; sealing defect

Below, we introduce a short description of each method and its main characteristics.

3.1.1   IEC 60599 method

This method classifies the anomalies according to Table 4. The ratios must be observed when one or more gases have high concentration or high growth. The input variables are the ratios R2, R5, and R1, and, instead of R1, you can also use C_2H_2/C_2H_6 [47].

Table 4. IEC method – Failures and the correspondent ratio limits [47].

Abbreviation	Failure	R2 (C2H2/C2H4)	R1 (CH4/H2) ou C2H2/C2H6	R5 (C2H4/C2H6)
PD	Partial Discharges	Negligeable value	<0.1	<0.2
D1	Low Energy Discharges	>1.0	0.1– 0.5	>1.0
D2	High Energy Discharges	0.6– 2.5	0.1– 1.0	>2.0
T1	Termal Failure T<300 ºC	Negligeable value	Negligeable value	<1.0
T2	Termal Failure 300ºC<T<700ºC	<0.1	>1.0	1.0 – 4.0
T3	Termal Failure T<700 ºC	<0.2	>1.0	>4.0

3.1.2   Duval method

Duval's method interprets dissolved gases through a triangle of relative percentages of CH4, C2H2, and C2H4 gases. The triangle is shown in Figure 12, where the different colored regions are associated with different faults. The relative percentage of each gas is obtained by dividing the quantity (in ppm) of the gas by the sum of the quantities of the three gases [51]. For example, to get the relative percentage of CH4:

$$\%CH_4 = \frac{CH_4}{CH_4 + C_2H_2 + C_2H_4}, \tag{1}$$

where CH_4, C_2H_2, and C_2H_4 represent the amounts of the respective gases in ppm.
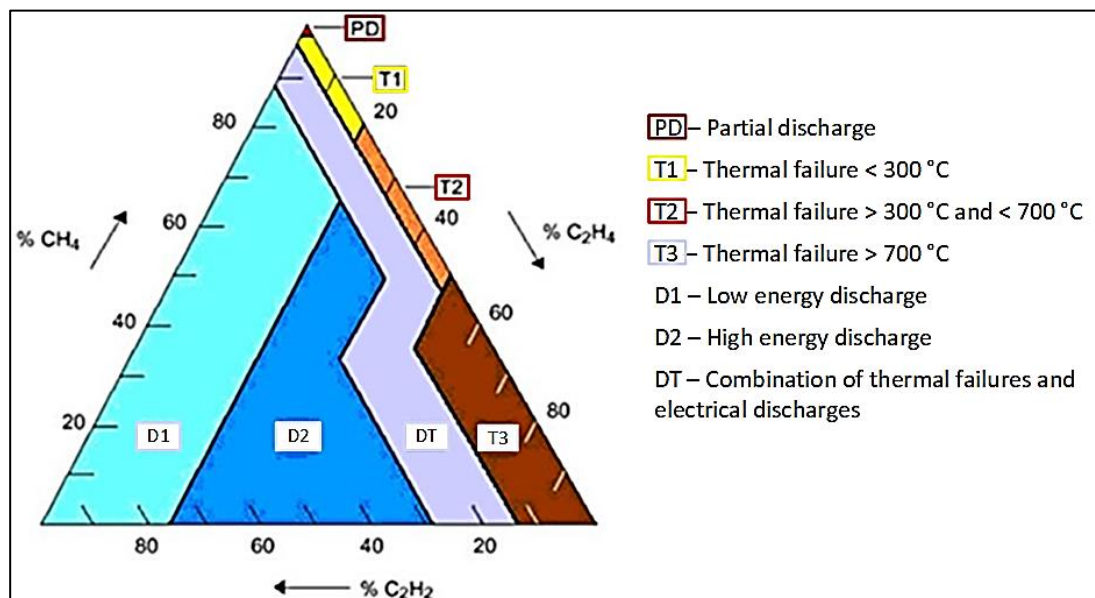
Figure 12 - Duval's triangle and associated faults [51].

3.1.3   Key gas method

The faults are qualitatively determined by the concentration of the different key gases (in ppm) based on the typical or predominant gases at various temperatures. In

Table 5, the classification of the types of failures according to the associated key gases is presented [47].

Table 5. Key Gas Method – Key gases and associated failures [47].

Key Gases	Failures	Typical emission proportion
H_2 e C_2H_2	High energy electrical discharge	Large amounts of H_2 and C_2H_2. Small quantities of CH_4 and C_2H_4. Formation of CO_2 e CO indicates paper combustion.
H_2	High energy electrical discharge, partial discharge	Mainly H_2. Small amounts of CH_4. Trace elements of C_2H_4 and C_2H_6.
C_2H_4	Oil overheating	Mainly C_2H_4. Reduced quantities of C_2H_6, CH_4, and H_2. Residues of C_2H_2, with large temperature failures.
CO	Paper overheating	Mainly CO and CO_2.
H_2	Electrolysis	Mainly H_2.

3.1.5   Doernenburg's method

This method suggests three types of faults: thermal, electric arc, and low-energy discharge (corona). This method only considers its use when the concentrations of H_2, CH_4, C_2H_2, and C_2H_4 exceed twice the established limits and the concentrations of CO and C_2H_6 gases exceed three times the established limits. However, the method is complex and often leads to "none interpretation" [47]. In Figure 13, the flowchart of the procedure to be carried out to obtain the transformer diagnosis is presented. The L_1 limit is specified for each gas and is shown in Table 6, being enough for one gas to exceed the limit to advance.
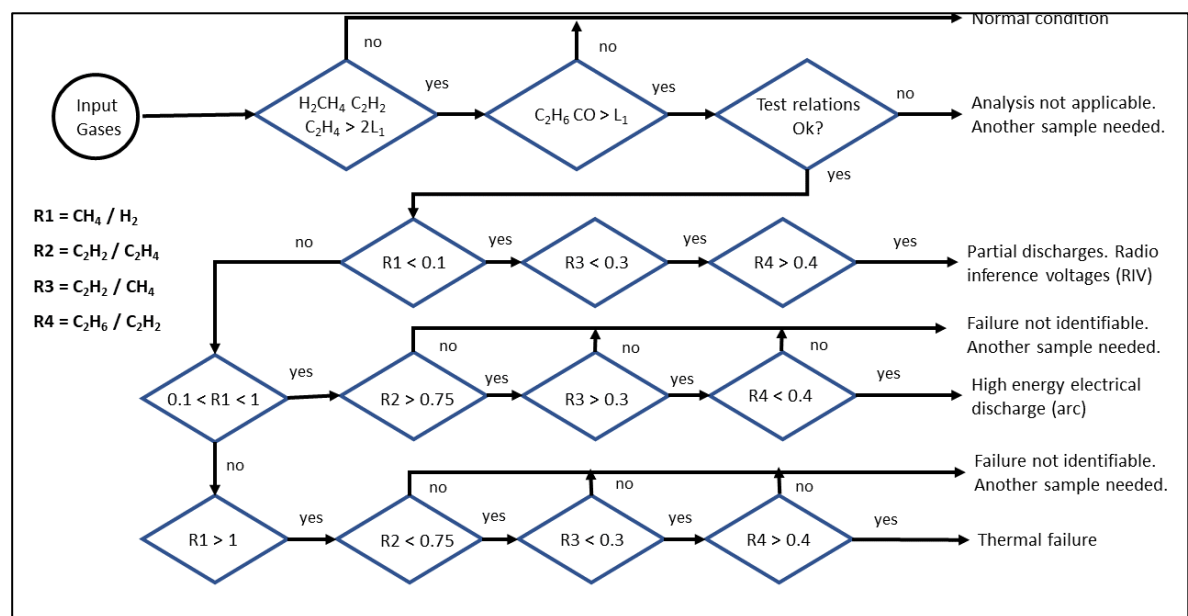
Figure 13 – Doernenburg's method – [47].

Table 6. Limit L_1 specified for each gas and its values that cannot be exceeded.

Gases	Limit L1 (ppm)
H_2	100
CH_4	120
CO	350
C_2H_2	35
C_2H_4	50
C_2H_6	65

3.1.6   TDCG Method ("Total Dissolved Combustible Gas")

This methodology is present in North America's history, as it had its initial application as an important tool in analyzing gases in mines [48]. It does not offer a diagnosis related to transformer failures. However, it is relevant in indicating the variation of gas levels. In ppm, the TDCG value is obtained from H_2, CH_4, C_2H_2, C_2H_4, C_2H_6, and CO gases, computing the augmenting rate by making the difference between the TDCG values of two samples divided by the time (days) between samples. The TDCG limits, sample intervals, and suggested operating procedures are presented in Table 7.

Table 7. TDCG Method - Limits and operating procedures [48].

TDCG level (ppm)	TDCG Generation Rates (ppm/day)	Sampling Intervals and Operating Actions for Gas Generation Rates	
		Sampling Interval	Operating Procedures
<720	<10	Twice a year	Continue normal operation.
	10-30	Quarterly	
	>30	Monthly	Caution is necessary. Analyze individual gases to find the cause. Determine load dependence.
721-1920	<10	Quarterly	Caution is extremely necessary. Analyze individual gases to find the cause. Determine load dependence.
	10-30	Monthly	
	>30		
1921-4630	<10	Monthly	Exercise extreme caution. Analyze individual gases to find the cause. Plan outage.
	10-30	Weekly	
	>30		
>4630	<10	Weekly	Exercise extreme caution. Analyze individual gases to find the cause. Plan outage.
	10-30	Daily	
	>30		Consider removal from service.

3.1.7 CO_2/CO ratio

The CO_2/CO ratio is usually used as an indicator of the thermal decomposition of cellulose, and only for ratio values lower than three should this indication be taken into account [42].

3.1.8   Rogers method

A simple method of diagnosing transformer faults. Its validity is based on the correlation of the results of many failures identified with the analysis of the gases in each

case. Table 8 summarizes how the corresponding associated faults are attributed, according to the values of the ratios chosen in this method.

Table 8. Rogers Method – Relationship between ratios and failures [46].

Ratio R1 (CH_4/H_2)	Ratio R2 (C_2H_2/C_2H_4)	Ratio R5 (C_2H_4/C_2H_6)	Failure
0.1-1.0	<0.1	<1.0	Normal operation.
<0.1	<0.1	<1.0	Low energy electrical discharge
0.1-1.0	1.0-3.0	>3.0	High energy electrical discharge
0.1-1.0	<0.1	1.0-3.0	Low temperature thermal failure
>1.0	<0.1	1.0-3.0	Thermal failure <700ºC
>1.0	<0.1	>3.0	Thermal failure >700ºC

3.2 *Oil quality*

Several tests are carried out on the oil to verify its contamination, deterioration status, and electrical properties. Electrical, physical, and chemical tests (dielectric strength, power factor, interfacial tension, color, sludge and sediment, acidity index, relative humidity, kinematic viscosity, and particle content, among others). Table 9 presents some of the methods and standards for each of the most important tests [52].

Table 9. Oil quality tests and standards/methods [52].

Test	Standard/ ASTM method	IEC
Color	ASTM D1500	ISO 2049
Interfacial voltage	ASTM D971	ISO 6295
Visual inspection	ASTM D1524	-
Breakdown voltage	ASTM D1816	IEC60156
Dissipation factor	ASTM D924	IEC247
Neutralizing number	ASTM D664	IEC62021
Water content	ASTM D1533	IEC60814

3.2.1 Color

This test allows you to gain insight into the state of the oil quickly. The evaluation is made by comparison with normalized standards, assigning an oil color number. Rapid color changes or high color numbers are associated with advanced aging and/or oil contamination [53].

3.2.2 Interfacial voltage

The interfacial voltage value, which determines the tension at the interface between two liquids (oil and water), indicates soluble polar contaminants in the oil [53].

3.2.3 Dielectric Breakdown Voltage

The dielectric breakdown voltage measures the oil's ability to withstand electrical voltages. The test is carried out by immersing two electrodes in oil at a distance, as shown in Figure 14. Subsequently, several levels of alternating voltage are applied until the break occurs. Contaminants such as water, sediment, and conductive particles reduce the breakdown voltage level [53].

Figure 14 - Dielectric breakdown voltage measurement test [36].

3.2.4   Dissipation factor

The dissipation factor measures the loss angle (tan δ) and indicates the leakage current flowing through the oil. With the deterioration or contamination of the oil, the value of the loss angle increases, and, for new oils, it is expected to obtain typical values lower than 0.005 [53].

3.2.5   Neutralizing number

The neutralizer number or acidity value is an indicator of the oxidation/decomposition of the oil. However, acids in the oil can also arise from outside sources such as a polluted atmosphere. These acids, together with water, can lead to corrosion inside the transformer [53].

3.2.6   Water content

The water content is a very important parameter to control, as it accelerates the insulation aging process and, at the same time, is one of the products resulting from this process. A more detailed explanation of this test and its importance is given in section 4.3.

3.2.7   Limits

Table 10 presents the limits suggested in [54] for some of the tests carried out to determine the quality of transformer oil.

Table 10. Transformer oil quality tests and their limits.

Test	Value according to voltage classes		
	≤ 69 kV	69 kV - 230 kV	≥ 230 kV
Dielectric breakdown voltage [kV] for 1mm electrode distance (minimum value)	23	28	30
Interfacial tension [mN/m] (minimum value)	25	30	32
Neutralizing number [mg KOH/g] (maximum value)	0.2	0.15	0.1
Water content [ppm] (maximum value)	35	25	20

3.3   *Degree of polymerization*

The degree of polymerization is defined as the number of glucose rings in a cellulose macromolecule (Figure 15). It provides an indication of the state of the paper and the mechanical stress of the insulation system. This can be measured indirectly through the analysis of furanic compounds or directly measured through paper samples.
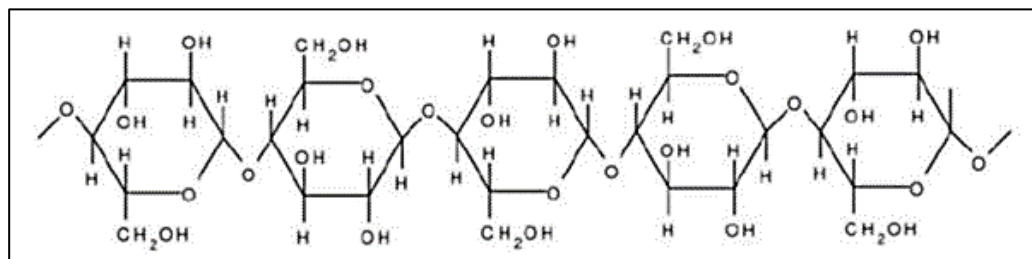
Figure 15 - Chemical structure of cellulose molecule [55].

The degree of polymerization is defined as the number of glucose rings present in a cellulose macromolecule. It indicates the paper's condition and the mechanical strength of the insulation system. This can be measured indirectly via an analysis of furan compounds or directly through paper samples. The Arrhenius equation (2) is used to estimate the degree of polymerization (DP) at a given time t after its initial measurement. It depends on activation energy (E_a), chemical environment (A), hotspot temperature (T), and gas constant (R).

$$\frac{1}{DP(t)} - \frac{1}{DP(0)} = A.e^{-\frac{E_a}{R.T}}.t = kt \tag{2}$$

Where

$DP(t)$ and $DP(0)$ correspond to the DP at time t and start, respectively.
A – constant that depends on the chemical environment.
E_a - activation energy of the reaction, in kJ/mol
R - perfect gas constant (8,314 J/mol/K)
T - absolute temperature, in K
k – speed constant (aging)

3.3.1   Analysis of furanic compounds

Furanic compounds are a group of organic components formed by the deterioration of cellulose material (paper) in the transformer. Overheating with moisture and oxidation accelerate paper deterioration, resulting in furanic compounds, which dissolve in the oil. An analysis by high-pressure, high-resolution liquid chromatography allows characterizing the degree of polymerization of cellulose indirectly.

The value of the degree of polymerization obtained through the analysis of furanic compounds refers to the average value of the entire solid insulation structure. As paper does not age uniformly, there may be regions where degradation is more severe. As described above, the high CO_2 and CO levels indicate the need to analyze furanic compounds. The five main types of furanic compounds that can form are:

    a) 2-furfuraldehyde (2FAL)
    b) 2-acetylfuran(2ACF)
    c) 2-furfuryl alcohol (2FOL)
    d) 5-methyl-2-furfuraldehyde (5MEF)
    e) 5-hydroxy-methyl-2-furfuraldehyde (5HMF)

The measurement of furanic compounds in mineral oil is carried out following the IEC 61198 standard. Several methods relate the degree of polymerization with furanic compounds found in the oil. We highlight the *Chendong* method [56] (eq. 3) applicable to transformers with kraft paper, the *Stebbins* method (eq. 4) [56], which results from a modification of the *Chendong* method for transformers with thermally improved paper, the *De Pablo* method (eq. 5) [56] which was developed based on the theory of cellulose chain splitting and the *Pahlavanpour* method (eq. 6) [56], which is a modification of the *De Pablo* method where it is considered that the aging of the paper is not uniform. It is assumed that 20% of the inner layers near the winding degrade at twice the speed, which

associates the degree of polymerization with the concentration of furanic compound 2FAL [56].

Chendong:
$$DP = \frac{1,51 - \log\left([2FAL]_{ppm}\right)}{0,0035} \tag{3}$$

Stebbins:
$$DP = \frac{1,655 - \log\left([2FAL]_{ppm}\right)}{0,0035} \tag{4}$$

De Pablo:
$$DP = \frac{7100}{8,8 + [2FAL]_{ppm}} \tag{5}$$

Pahlavanpour:
$$DP = \frac{7100}{8,8 + [2FAL]_{ppm}} \tag{6}$$

3.3.2   Direct measurement through paper samples

To directly determine the degree of polymerization, a paper sample is required. However, it is necessary to take the transformer out of service. The value is obtained by viscosimetric measurement according to the IEC 60450 standard. Once again, the value obtained cannot be generalized for the entire winding.

3.4   *Frequency response analysis*

With the analysis of the transformer's frequency response, it is possible to detect any deformations in the windings by comparison with a previously obtained frequency response reference. Differences in resonance frequency or magnitude are related to changes in inductances and capacities, which are defined according to the physical dimensions and materials of the transformer. This frequency response is obtained by imposing a voltage pulse at the transformer's input and measuring the frequency spectrum of its response at the output obtained by the Fourier Transform. This method, however, requires taking the transformer out of service. However, there are currently attempts to carry out this test in service, in which electrical transients that already exist in the electrical network are used. This measurement is currently simple to perform. However, the interpretation of the results is a little complicated, and a consensus is often not reached [34], [4].

3.5   *Power factor*

Power factor or loss factor is an important measure in monitoring the condition of the transformer and crossovers. The power factor refers to the quotient between the leakage current of the resistive component and the capacitive component, which result from the application of an alternating voltage. If the insulation were perfect, the capacitive component of the current would naturally be in advance of 90° relative to the voltage. However, as there are Joule losses, this advance is less than 90°, as the resistive component increases with the deterioration of the dielectric. This test is done to determine the insulation condition between windings and compartments, and it only indicates the general state of the insulation system [40].

3.6   *Excitation current*

The measurement of the excitation current, performing a no-load test, allows the identification of faults in the magnetic circuit and the windings of single-phase or three-phase transformers, such as short-circuited windings open-circuit problems in the voltage regulator, and also failures in the electrical connections. When any of these problems occur, the reluctance of the magnetic circuit changes, which affects the current needed to impose a magnetic flux on the core. Test results should be compared with previous tests or other phases (in the three-phase) [4].

3.7   *Leakage reactance*

Also called short-circuit testing, leakage inductance measurement is a traditional method to detect changes in winding geometry and the core. These deformations alter

the magnetic flux and, consequently, the leakage inductance. The values obtained are compared with information from the nameplate, previous tests, or similar transformers [4].

3.8 *Electrical insulation resistance*

This test is usual. However, it is not standardized due to the variability of results depending on the environment at the time of measurement (temperature, humidity, level of impurities in the insulation materials). The electrical insulation resistance provides information about its state [4].

3.9 *Electrical resistance of windings*

The electrical resistance of each winding is measured in direct current. It is necessary to measure and record the temperature associated with each resistance measurement, as the temperature varies the resistance. This test indicates the status of the windings and the voltage switch. A variation of more than 5% with respect to the information on the nameplate indicates serious damage to the conductor [4].

3.10 *Partial electrical discharges*

The partial discharge test is essentially qualitative. Partial discharges result from local dielectric disruptions in the insulation system. The intensity and frequency of partial discharges are a good indicator of the state of the insulator, as they increase along with the corrosion and decomposition of the insulating material. Partial discharges generate electromagnetic waves, acoustic waves, local overheating, and chemical reactions. To understand its location, both acoustic and electrical signals must be measured. There is already some continuous monitoring equipment based on the measurement of these two variables [41].

3.11 *Relationship between turns*

Coils are subject to electrical and mechanical wear, which can cause short circuits or open circuits. The ratio of the number of turns (N2/N1) is related to the quotient between the secondary voltage (V2) and the primary voltage (V1), that is, V2/V1≈N2/N1. The value of the ratio between turns must not deviate more than 0.5% from the ratio between the nominal voltages of the windings stipulated on the nameplate.

3.12 *Return voltage and polarization currents*

The restoration voltage method allows access to the water content and insulation system's degradation level. This test is carried out by charging the insulator's dielectric structure with electrical charges by applying a voltage pulse, then creating a short-circuit through an external impedance. The signal obtained when removing the external impedance allows characterizing the state of the insulation system. By analyzing the frequency response of the polarization and depolarization currents, it is also possible to perceive the condition of the insulating material [4].

3.13 *Mechanical vibrations*

Transformer vibrations originate in the core, induced by magnetostriction (change in the shape of the ferromagnetic material due to a change in the magnetic field which leads to core vibration), and vibrations in the windings, induced by electromagnetic forces (interaction force between the current of the windings and the dispersion field, resulting in its vibration of the windings). The excitation frequency of the core and windings is twice the frequency of the alternating current, as the forces vary with the square of the voltage and the current of the electrical signal, respectively. It is also known that the core presents vibration frequencies of greater magnitude due to the non-linearities of the core's magnetostriction.

To measure these vibrations, sensors (accelerometers) are installed on the sides and top of the transformer tank. Several sensors are placed to reduce uncertainty due to the dimensions and complexity of the transformers. The obtained signals are generally transmitted through an optical cable and registered in a specific device. With these signals, it is then possible to detect the condition of the windings and the magnetic circuit [42].

3.14 Temperature

The load capacity of transformers is limited by the temperature of the windings (which is not uniform). The traditional method for estimating the temperature of windings is to measure the temperature at the top and bottom of the tub. The real limiting factor is the "hot spot" located on top of the transformer that is not directly accessible. Sensors have been developed to directly measure the temperature of the "hot spot" of the windings, the most reliable of which seem to be fiber optics. These sensors are placed on the spacers or on the conductors to be monitored. The hot spot temperature, according to IEC, must not exceed 98°C [41].

3.15 Infra-red test

Direct monitoring via thermographic images obtained by infrared testing is important to prevent abnormal operating conditions and protect the insulation material. The high temperatures in the transformer, especially the "hot spot," contribute to oil decomposition, paper deterioration, and power losses. With this test, it is possible to locate the hot zones at a temperature higher than the external surface of the transformer. Four colors are displayed in the thermal image: white, red, blue, and black. Warmer zones appear in white and red and cooler zones in black and blue [34].

3.16 Bushings condition

Transformer bushings are one of the most frequent causes of breakdowns in it, and in most cases, the breakdowns result from water ingress. Those in contact with the outside suffer greater deterioration and are more vulnerable to external accidents. The techniques used to monitor the transformer bushings are adaptations of the abovementioned techniques (analysis of gases dissolved in oil, oil quality, partial discharges, infrared thermography, power factor, temperature, etc.) [4].

3.17 Tap-changer condition

The transformer's voltage regulator can focus on various abnormal operating conditions. Adding to this, the voltage regulator is one of the few transformer elements that perform mechanical movements. It is subject to greater wear. As such, monitoring this type of apparatus is essential. The monitoring and analysis of the temperature in the resistance of the motor windings of the power supply that drives the commutator, the gases dissolved in the oil, and its vibration pattern stand out [4].

4. Online diagnostic models for power transformers

After reviewing the diagnostic methodologies of power transformers, it is interesting to understand which ones have monitoring applications automatically and continuously over time and how they can be applied. Monitoring is done through multiple sensors that capture some variables that make it possible to determine the status of the transformer and its components.

Continuous monitoring overtime automatically allows companies that have transformers to monitor the status of their assets "minute-by-minute," as such, it has the advantage of allowing early detection of anomalies, preventing them from evolving into situations with large technical and economic losses.

4.1   Thermal model

It is essential to monitor the temperature of the transformer, especially the hotspot, which is somewhere on the top of the transformer, as shown in Figure 16, to increase operating efficiency and reduce the probability of transformer shutdown. Another important measure of temperature is the top oil, which represents the temperature at the top of the transformer oil. It is possible to obtain the hot spot temperature directly, through a fiber optic system, or indirectly, through models that estimate it.

The calculation of the hot spot temperature, according to [43], is essentially based on the diagram in Figure 16, which is based on the following hypotheses:

1. The oil temperature in the transformer tank increases linearly between the bottom and the top, regardless of the type of cooling;
2. The temperature along the winding also increases linearly between the bottom and the top, regardless of the type of cooling. For the same horizontal position, this temperature always exceeds that of the oil by the value of a constant gr (gradient between the average temperature of the windings and the oil);
3. The temperature rise of the hot spot is greater than the temperature rise of the winding on top of the winding. The difference is determined by multiplying the constant gr by the hot spot factor (HSF).
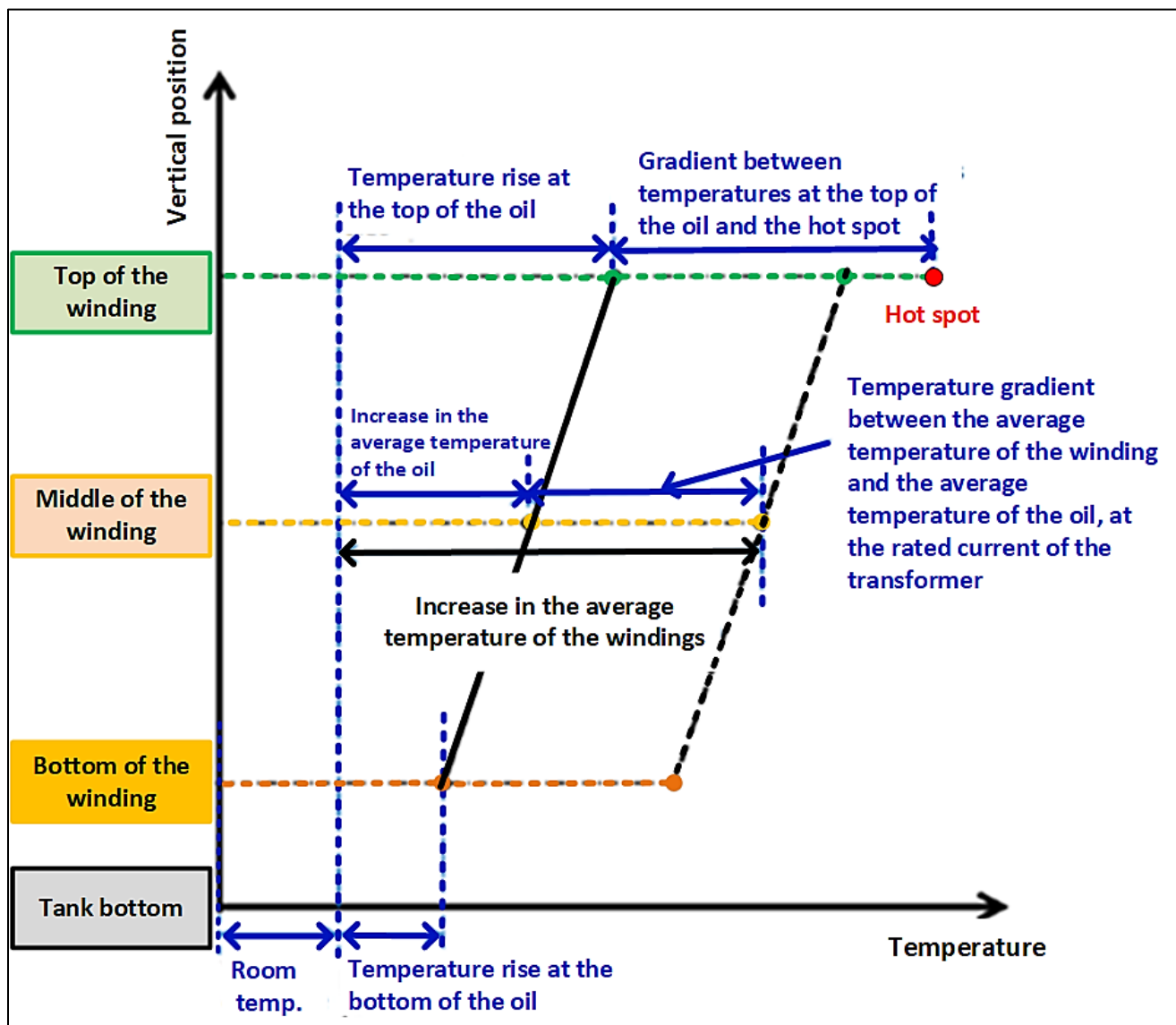

Figure 16 - Diagram for the thermal model of the power transformer [43].

In [43], it is indicated that it is possible to estimate the temperature at the top of the oil (θ_0) through equation (4.1), which depends on the ambient temperature (θ_a), the load factor (K), which is calculated by dividing the rms value of the current at its nominal value, the ratio between the load losses at the nominal current and the no-load losses (R), the exponent of the total losses versus the increase in temperature at the top of the oil (x), the increase in steady-state temperature under nominal loss conditions ($\Delta\theta_{or}$), the average of the oil's thermal time constants (τ_0) and the thermal model constant (k_{11}).

$$\left[\frac{1+K^2.R}{1+R}\right]^x . (\Delta\theta_{or}) = k_{11}.\tau_0.\frac{d\theta_0}{dt} + [\theta_0 - \theta_a] \tag{7}$$

To obtain the hot-spot temperature (θ_h), it is necessary to add to the top oil temperature (θ_0) the gradient between the hot-spot temperature and the top oil temperature with the considered load ($\Delta\theta_h$). To facilitate the calculation of this gradient, it is divided into two differential equations (4.3) and (4.4), and then the resulting gradients, $\Delta\theta_{h1}$ and $\Delta\theta_{h2}$ (equation (4.2)), is added.

$$\Delta\theta_h = \Delta\theta_{h1} - \Delta\theta_{h2} \tag{8}$$

$$k_{21}.K^y.(\Delta\theta_{hr}) = k_{22}.\tau_w.\frac{d\Delta\theta_{h1}}{dt} + \Delta\theta_{h1} \tag{9}$$

$$(k_{21} - 1).k^y.(\Delta\theta_{hr}) = \frac{\tau_0}{k_{22}} .\frac{d\Delta\theta_{h2}}{dt} + \Delta\theta_{h2} \tag{10}$$

The remaining symbols of variables or parameters that appear in these three equations are the thermal model constants (k_{21} and k_{22}), the winding time constant (τ_w) and the current exponent versus the winding temperature rise (y).

For normal charge cycles, the maximum oil top temperature is 105ºC, and the hot spot temperature is 120ºC. The standard also suggests values for the characteristic parameters of the power transformer according to the type of cooling, which are presented in Table 1 [43].

Table 11. Transformer oil quality tests and their limits for different cooling methods.

Test measure	ONAN ("Oil natural air natural")	ONAF ("Oil natural air forced")	OF[a] ("oil forced")	OD[b] ("oil-directed")
x	0,8	0,8	1,0	1,0
y	1,3	1,3	1,3	2,0
R	6,0	6,0	6,0	6,0
τ_0 (min)	210	150	90	90
τ_w (min)	10	7	7	7
$\Delta\theta_{or}$ (K)	52	52	56	49
$\Delta\theta_{hr}$ (K)	26	26	22	29
k_{11}	0,5	0,5	1,0	1,0
k_{21}	2,0	2,0	1,3	1,0
k_{22}	2,0	2,0	1,0	1,0

(a) OF includes OFAN, OFAF, OFWF cooling types.
(b) OD includes ODAN, ODAF, ODWF cooling types

An example of calculation using the differential equations in (4.1), (4.3), and (4.4) is described in [43], which emphasizes the fact that the sampling time must be lower than

half the time constant of the windings (τ_w), which is in the order of 7 minutes. Thus, the sampling period should be less than 3 minutes. If there is still information on the type of cooling at each moment, the constants must correspond to this one. In other words, if the transformer is ONAN in an instant, for calculation purposes, the constants referring to this type of cooling must be used. If at another moment the type of cooling changes to ONAF, the constants must be changed according to the table to those that correspond to ONAF cooling.

4.2 *Model for estimating water content in insulation (paper and card) and temperature of water bubbles*

The condition of the insulation is an essential aspect in the reliability of transformer operation, as transformers with high water content in the paper have a higher aging rate (acceleration of paper decomposition) and cannot withstand, without risk, higher loads since there is a greater possibility of bubble formation [44]. These are formed when there is an increase in temperature, causing the absorbed water to evaporate with high steam and pressure in the inner layers of the paper. If the pressure is too high, it leads to the expulsion of oil from the paper layers and the formation of bubbles on the surface of the insulation, leading to a decrease in the dielectric capacity [45].

The water in power transformers is mostly dissolved and can move between oil and solid insulation. However, some water is associated with by-products resulting from oil oxidation, which is only partially available for migration. Most water is found in solid insulation (paper and cardboard). The average water content in it is almost constant under normal conditions over time, the opposite being true for oil. An example of the water content distribution in a 25 MVA transformer [46] is presented in Table 12, in which the above is illustrated.

Table 12. Water distribution in a 25 MVA transformer for different temperatures.

Insulation	40°C		80°C	
Oil (25000 l)	10 ppm	0,25 kg	80 ppm	2,0 kg
Paper (2500 kg)	3 %	75 kg	2,93%	73,25 kg
Total		75,25 kg		75,25 kg

Water appears in the transformer through three distinct sources [47]:
• Residual water that comes from manufacturing – During manufacturing, water is installed in the different components of the transformer and, despite drying, there is always a portion of water that remains, typically 0.4-1%;
• Entry from the atmosphere – The atmosphere is considered the main source of water for transformers, which can enter, for example, by exposure to humid air during installation or repairs and due to cracks that expose the inside of the transformer;
• Aging of oil and cellulose – The decomposition of cellulose, which essentially consists of breaking the bonds of glucose chains, is reflected in the appearance of water and other compounds. Oil oxidation also contributes to water formation. The normal annual water increase is approximately 0.1% [47].

Measurement methods

There are several ways to measure water content on paper, divided into direct and indirect. The direct measurement method extracts a paper sample and is performs Karl Fischer titration [47]. To access the water content of the paper or cardboard insulation indirectly, one takes samples from the water content in oil or measures electrical quantities, such as the power factor or the dielectric response. The simplest and most

common method is measuring the water content in oil. The methodology consists of three steps:

- Obtaining an oil sample from the transformer in service;
- Measurement of water content in oil (ppm) through Karl Fischer titration;
- Estimation of water content in paper or board insulation (%) using equilibrium curves. Figure 17 shows an example of these curves published by Oomen in 1984 [46].
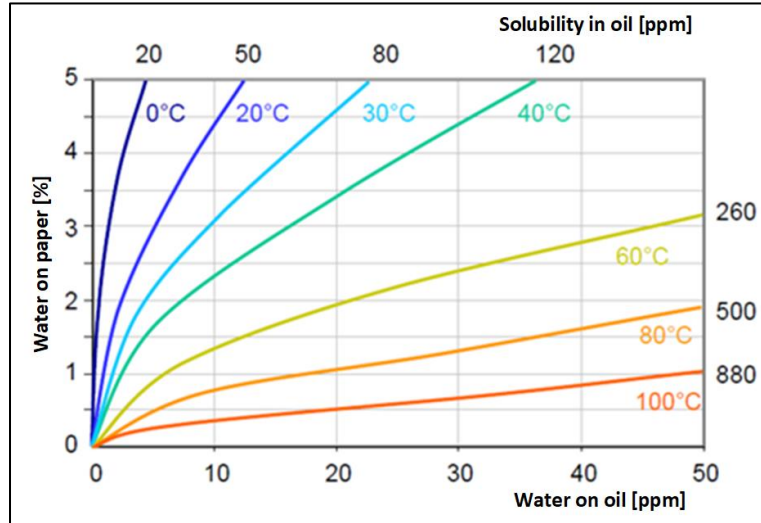
Figure 17 – Oomen equilibrium curves, adapted from [47].

The applicability of these curves is subject to thermodynamic equilibrium. However, in practice, thermal stability conditions are never achieved. In addition to transformer load variations, the transformer is subjected to daily and seasonal temperature variations. Thus, balance curves cannot be directly applied. Other relevant errors are described in [47], such as: obtaining different results using different curves and the existence of different water contents along the winding due to the temperature gradient.

Calculation of water content in the paper

To estimate the water content of the paper, it is common to use the Fessler equation (11) [46]. He combined data from Houtz, Ewart, Oomen, and their experiment [48] to obtain an equation that allows estimating the water content in the paper (WCP) through temperature (T) and water vapor pressure (p) exercised by the role.

$$WCP = 2,173.\,10^{-7}.\,p^{0,6685}.\,e^{\frac{4725,6}{T+273,15}} \qquad (11)$$

Through the definition of relative saturation (RS) [45], it is possible to associate the pressure (p) with the water-in-oil content (WCO). Equation (4.6) represents the relative saturation of an ideal gas or liquid and is defined as the ratio of WCO and water-in-oil solubility (WS). In contrast, equation (12) refers to a solid and is defined as the ratio between the water vapor pressure (p) exerted by the paper and the saturation water vapor pressure (p_S) [45].

$$RS = \frac{WCO}{W_S}.\,100\% \qquad (12)$$

$$p_{celulose} = p_{óleo} = p_{ar} \qquad (13)$$

Under thermodynamic equilibrium conditions, which are obtained when thermal, mechanical, and chemical equilibrium is reached, the migration of water molecules

within the materials and the migration between oil and cellulose tends to zero [45]. This corresponds to equal vapor pressure in the different materials (equation (4.8)).

$$RS = \frac{p}{p_S}.100\% \qquad (14)$$

Thus, under these conditions, the relative saturation also takes the same value in different adjacent materials, as indicated in equation (15).

$$RS_{celulose} = RS_{óleo} = RH_{ar} \qquad (15)$$

Using the equality of (15) in (12) and (13), we obtain:

$$\frac{WCO}{Ws} = \frac{p}{p_S} \qquad (16)$$

The solubility of water in oil (WS) is calculated using equation (17) [45].

$$W_S = 10^{-\frac{B}{T+273.15}+A} \qquad (17)$$

In [25], it is suggested that B takes the value of 1567 and A the value of 7.0895. However, parameters A and B vary depending on the oil and its condition.

To determine the water vapor pressure, it is also necessary to calculate the saturation water vapor pressure. In 1981, Buck [49] came up with an expression for its calculation (4.12).

$$p_S = 0,00603. e^{\frac{17,502 \times T}{240,97+T}} \qquad (18)$$

It is concluded that the water vapor pressure is estimated by equation (19), which results from the substitution of (17) and (18) in (16).

$$p = \frac{WCO}{10^{-\frac{B}{T+273,15}+A}} * 0,00603 * e^{\frac{17,502 \times T}{240,97+T}} \qquad (19)$$

Finally, the water content of the paper is estimated by substituting (19) for (11). As seen before, this value has some inherent errors, which can be reduced by making a long-term average, thus obtaining an approximation of the equilibrium condition [47].

It is proved in [49] that an average of seven days offers a good accuracy of the water content in solid insulation for those seven days. That is, weekly averages are recommended. It is also suggested that by making a moving window average of the seven previous days, it is possible to obtain valid values of daily water content instead of weekly.

Temperatures considered in the previous equations.
The temperatures of the equations vary, and for equation (17), the temperature must be the temperature at the oil harvesting site for measuring the water content in the oil (Temperature 3 in Figure 18), the temperature of the other equations is associated with the temperature of the paper. The water content of the paper at the bottom (WCP 2) or top (WCP 1) can be estimated. The temperatures to be used are the lower part (Temperature 2) and the upper part (Temperature 1). The water content in the paper will be higher in the lower part of the transformer since the temperature is lower there, so there is less water transfer into the oil. However, there is a greater risk of forming bubbles in the upper part because the temperature is higher.
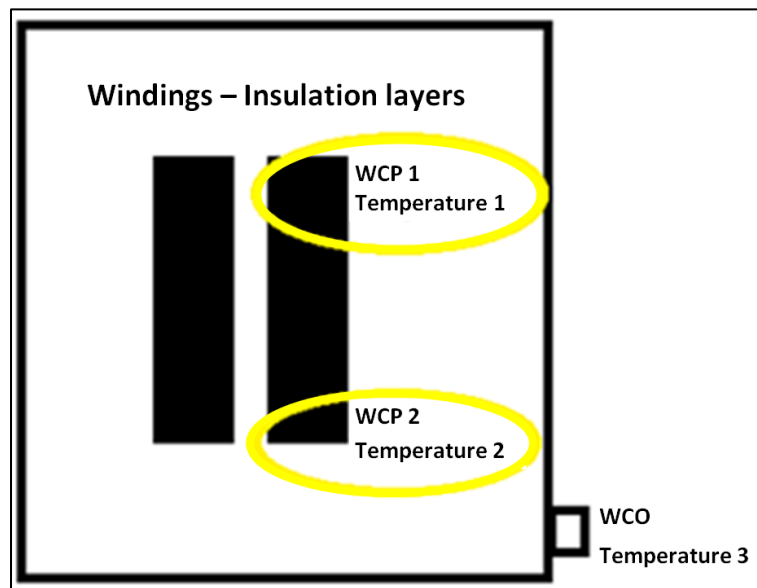
Figure 18 –Temperatures for calculating water content in solid insulation.

Limits and definitions.

The IEEE C57.106-2002 standard suggests maximum percentages of water in the solid insulation system [25] depending on the transformer voltage rating:
- <69 kV, 3% maximum
- 69 kV-230kV, 2% maximum
- >230 kV, 1.25% maximum

Other existing standards only assign ratings for water content. For example, in [46], the IEEE 62 – 1995 standard recommends the following attribution of water percentages:
- Dry insulation, 0 - 2%
- Wet insulation, 2 - 4%
- Very wet insulation, >4.5%

Limits and definitions.

An important measure to monitor the water content of the paper is the temperature at which water bubbles can occur. In [44], two relations that allow calculating the temperature of origin of water bubbles are referred to. The first (20) is an empirical formula suggested by Oommen and Lindgren [44], depending on the WCP, the total pressure acting on the bubbles (P), and the total gas content in the oil (g).

$$T = \left[\frac{6996,7}{22,454 + (1,4495.\ln(WCP)) - \ln(P)} \right] - \left[e^{0,473*WCP} * \left(\frac{g}{30} \right)^{1,585} \right] \tag{20}$$

The other equation (21) was published by Koch and Tenbohlen [44] and uses two parameters that depend on the material (*A* and *B*) and the WCP. Some typical values of these parameters are available in Table 13, which depend on the type of oil and the condition of the insulating kraft paper.

$$T = A \times e^{B*WCP} \tag{21}$$

Table 13. Parameters to be used in equation (4.21)

Oil	Paper	A	B
Shell Diala D (new)	New	195,5	-0,11186
Shell Diala D (new)	Improved, thermically new	237,7	-0,13718
Shell Diala K 6 SX (used)	Improved, thermically used	178	-0,07338

4.3 *Transformer Aging Model*

The aging model aims to estimate the state of solid insulation over time, which is extremely useful since there is no direct access to solid insulation instead of liquid insulation.

It is possible, as mentioned above, to estimate the degree of polymerization of the solid insulation after t years after its determination from equation (3.2). It is also possible to determine the remaining lifetime by imposing a final polymerization degree, generally 200.

The activation energy of the reaction (Ea) takes as its expected value 111 kJ/mol. The constant that depends on the chemical environment (A) varies with water content, oxygen content, and acidity, the latter being less important. It is possible to update the estimate of the degree of polymerization depending on the sampling time of temperature, water content, and oxygen content. The temperature will be the hot spot, considered the worst case.

In [50], the value of the constant A was determined for low, medium, and high oxygen concentration, all for WCP of 0.5%, 1.6%, and 2.7%, and two types of paper, kraft, and thermally improved kraft, the determined values are shown in Table 14. From here, it is possible to determine the equations that enable the calculation of the constant A for thermally improved kraft paper by polynomial interpolation [51], as it was done for equations (22), (23), and (24), the equations obtained are (25), (26) and (27).

Kraft paper.
- Low oxygen content in oil (O_2 < 6000 ppm):

$$A = 1,78.10^{12}.\left(\frac{WCP}{100}\right)^2 - 1,10.10^{10}.\left(\frac{WCP}{100}\right) + 5,28.10^7 \tag{22}$$

- Average oxygen content in the oil (7000 ppm < O_2 < 14000ppm):

$$A = 1,30.10^{11}.\left(\frac{WCP}{100}\right) - 1,84.10^8 \tag{23}$$

- High oxygen content in oil (16500 ppm < O_2 < 25000 ppm):

$$A = 1,71.10^{11}.\left(\frac{WCP}{100}\right) + 1,55.10^8 \tag{24}$$

Thermally improved Kraft paper.
- Low oxygen content in oil (O_2 < 6000 ppm):

$$A = 2,26281.10^{12}.\left(\frac{WCP}{100}\right)^2 - 2,9119.10^{10}.\left(\frac{WCP}{100}\right) + 1,56625 * 10^8 \tag{25}$$

- Average oxygen content in the oil (7000 ppm < O2 < 14000ppm):

$$A = 3,13223.10^{12}.\left(\frac{WCP}{100}\right)^2 - 1,7686.10^{10}.\left(\frac{WCP}{100}\right) + 2,13124.10^8 \tag{26}$$

- High oxygen content in oil (16500 ppm < O₂ < 25000ppm):

$$A = 2,6405.10^{12}.\left(\frac{WCP}{100}\right)^2 + 9,0095.10^{10}.\left(\frac{WCP}{100}\right) - 8,74876.10^8 \tag{27}$$

Table 14. Constant *A* depends on water content, oxygen concentration, and paper type [50].

Paper type	Oxygen concentration in oil	Water content on paper	*A*
Kraft paper	Low	0,5%	$1,42.10^8$
		1,6%	$6,80.10^8$
		2,7%	$1,65.10^9$
	Average	0,5%	$4,66.10^8$
		1,6%	$1,66.10^9$
		2,7%	$3,33.10^9$
	High	0,5%	$9,33.10^8$
		1,6%	$3,05.10^9$
		2,7%	$4,70.10^9$
Thermally improved kraft paper	Low	0,5%	$6,92.10^7$
		1,6%	$2,61.10^8$
		2,7%	$1,03.10^9$
	Average	0,5%	$2,70.10^8$
		1,6%	$7,32.10^8$
		2,7%	$2,03.10^9$
	High	0,5%	$4,29.10^8$
		1,6%	$2,03.10^9$
		2,7%	$4,27.10^9$

4.4   *Load factor monitoring model*

The load factor model is quite simple, and its purpose is to monitor the transformer load factor, which, as suggested in [43], should be lower than 200%. The load factor calculation is performed by dividing the rms value of the current by its nominal value. Whenever the load exceeds 200%, an "alarm should sound," and one should look at the status of the transformer components and understand their operating condition. Note that the load factor is used as an input variable for the thermal model.

4.5   *Analysis model of gases dissolved in oil*

This model involves applying the methods of analysis of gases dissolved in oil already described in section 3.2. As previously mentioned, these are only valid when the concentration of one of the gases or the rate of change of one of the gases exceeds certain values. Table 15 summarizes the limits according to some of the most relevant standards or entities currently on the market. For "IEC Std 60599-97," the values considered normal are presented, while the maximum suggested limit is presented for the others.

Table 15. Limits for the concentration of gases dissolved in oil [52].

Standard	Gas concentration [ppm]							
	H_2	CO	CO_2	CH_4	C_2H_6	C_2H_4	C_2H_2	TCG
IEC Std 60599-97	60-150	540-900	5100-13000	40-110	50-90	60-280	3-50	-
Cigre 15.01	100	◎ CO+CO_2 < 10000		-	-	-	20	-
		◎ C_nH_y < 500						-
IEEE Std C57,104-91	100	350	2500	120	65	50	1	720
Laborelec	200	-	-	◎◎C_nH_y < 300				-

According to the IEC 60599-1999 standard, the slew rate limits are highly dependent on the type of transformer, the age, the type of identified faults, load patterns, and the oil volume. It is suggested that a 10% gas increase per month is generally indicative of an active fault and that if there is no variation or the variation is very small (<10% in a month), the fault has possibly disappeared. A study case applied the analysis methods of the gases dissolved in the transformer oil above their normal concentration. It noticed a variation above 10% when comparing the day under analysis with the day 30 days before.

4.6. *Model for monitoring and diagnosing crossings*

The diagnosis of the condition of the capacitive type crossings can be made through several tests. The most common practices in monitoring applications are measuring the dielectric loss factor (tg δ), the capacity (C), and the partial discharge test. For OIP type crossings, it is possible to analyze the gases dissolved in the oil and analyze their quality, such as in the oil in the transformer tank, stressing the tolerable limits, and the interpretation methods vary a little.

It is possible to detect material damage, such as cracks or breaks, or even short-circuited layers, the capacity increase or partial discharges can identify that. However, to detect by-products resulting from the aging of the crossing, such as water, it is advisable to monitor the dielectric loss factor [53]. It should be noted that for RBP type bushings, an increase in capacity can mean an oil impregnation. Two experimental tests were conducted to model the crossing monitoring: the measurement of the capacity C and the dielectric loss factor tg δ to detect abnormal operating conditions due to its simplicity and common use in the industry.

For continuous measurement of the values of C and tg δ, a sensor is placed in the capacitive socket that allows the connection of test equipment, as shown in Figure 19.

Figure 19 – Crossing monitoring sensor [54].

IEEE C57.19.01-2000 suggests threshold values for the power factor (compared to the nameplate value) and good power factor and capacity value changes before and after the dielectric breakdown voltage test. Table 16 lists these values.

Table 16. Limits for power factor and capacity change in different types of crossing.

Type of bushings	Power factor (cos θ) corrected to 20°C		Capacity
	Limit [%]	Acceptable change	Acceptable change [%]
OIP	0,5	+0,02/-0,04	±1,0
RIP	0,85	±0,04	±1,0
RBP	2,0	±0,08	±1,0

The weather where the transformer is installed should be considered when interpreting the values obtained for the power factor because it can be influenced by rain [55]. It can be seen in Figure 20 the evolution of the change in Δtg δ (blue) and the rainfall measured in three meteorological stations located next to the transformer (orange, red, and purple). Furthermore, the power factor varies with temperature, converting to a common temperature base, usually 20°C.
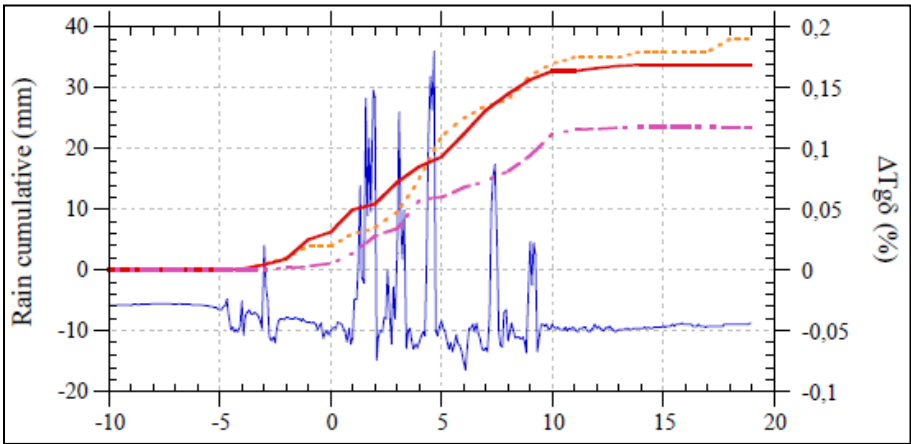

Figure 20 – Evolution of the change in the dielectric loss factor (Δtgδ) depending on the amount of rain measured in 3 weather stations near a power transformer [55].

4.7. *Model for on-load voltage regulator monitoring and diagnosis*

Of the existing methods to determine the operating condition of the voltage regulator on load, the most common in the industry that has applicability for continuous monitoring in time and automatically is: vibration measurement, motor current measurement, temperature measurement of your oil, analysis of the gases dissolved in your oil and also in the registration of its positions.

The analysis of the gases dissolved in the oil and their quality is similar to the transformer tank. For the on-load voltage regulator, as for the crossings, the interpretation methods and the tolerable limits are different.

Temperature is an important indicator of the operating condition of the on-load voltage regulator, as temperatures close to or above the tank generally indicate internal problems. However, the temperature is normal for some types of voltage regulators operating above the tank [56].

Table 17. Sensitivity of tests for detecting anomalies. Adapted from [55] and [57].

Abnormal operating conditions	Measurements/Testes					
	Temperature	Analysis of gases dissolved in oil	Motor electric current	Vibrations		
				Resistance	Reactance	Vacuum
Contact wear				X	X	X
Overheating	X	X		X	X	X
Transition timing				X	X	X
Alignment contacts			X	X	X	X
Electric arc		X		X	X	X
Sequence/Timing				X	X	X
Motor			X			
Brake			X			
Lubrication			X			
Control/Relays			X			
Connections / Gears			X	X	X	X

Table 17 summarizes the method's sensitivity for detecting voltage regulator failures. Green color corresponds to excellent/very good sensitivity, yellow to good/fair and red to poor sensitivity. For all measurements/tests, except for mechanical vibrations, the sensitivity is the same for all types of regulators. For mechanical vibrations depending on whether the transformer uses resistance or reactance in switching or a vacuum type, the sensitivity changes according to the type of abnormal operating condition to be detected.

By analyzing Table 17, it is concluded that by monitoring vibrations, oil temperature, and engine current, it is possible to determine the operating condition of

the on-load voltage regulator. Along with these three measurements, it is vital to know which position the contact is. Its position will also be one of the measurements for this model.

4.9. *Cooling system monitoring model*

The cooling system is monitored by comparing the measured hot spot and top oil temperatures with temperatures estimated by the thermal model. Knowing which type of cooling the transformer is at any given moment, it is possible to estimate the hot spot temperatures and the top of the oil by the thermal model and compare them with the measured temperatures. If temperatures are very different, it probably means that the cooling system is not working normally.

5. Conclusion

This paper reviews and analyses continuous methods of monitoring and diagnosis of large power transformers and summarizes the most important techniques that enable their implementation. It discusses in detail the reasoning of traditional methodologies for diagnosing power transformers, verifying the existence of different techniques to determine the condition of each of the main components.

It can be concluded that those methods represent a strong asset for entities that manage energy networks, as they allow them to have continuous access over time and automatically to the condition of their power transformers. These entities can act when an anomaly occurs in the transformer, avoiding technical and economic costs that can be quite high and even better managing the transformer's life cycle.

It will be interesting to relate the transformer's internal variables with external variables in the future with more data. For example, several cases indicate a strong relationship between transformer temperature, ambient temperature, and wind speed. Through weather forecasts, it could be possible to predict the temperature rate evolution of the transformer. It will also be interesting to try to develop a model for monitoring the windings that involve monitoring the ratio of the number of turns as a load function. As well as, with the power transformer's history, namely failures that have occurred and with the access of continuous data over time, it can be possible to associate them and remove patterns to predict the occurrence of failures. These are then suggested future directions that can bring novel methodologies in this area.

6. References

1. CIGRE Technical Brochure 248. (2004, June). Economics of transformer management.

2. Office of Electricity Delivery & Energy Reliability. Large Power Transformers and the U.S. Electric Grid; Office of Electricity Delivery & Energy Reliability: Washington, DC, USA, 2012.

3. "Large Power Transformers from Korea," USITC, Publication 4256, September 2011.

4. Westman T., Lorin, P. A., Ammann, P. A.. Keeping aging transformers healthy for longer with ABB TrafoAsset Management – Proactive Services, ABB Review 1/2010, 63 – 69.

5. CIGRE WG 12-05. (1983). An international survey on failures in large power transformers. ELECTRA, 88, 21-48.

"Special Report: Large Power Transformers and the U.S. Electric Grid," the Infrastructure Security and Energy Restoration Office of Electricity Delivery and Energy Reliability, U.S. Department of Energy, June 2012, https://www.energy.gov/sites/prod/files/Large%20Power%20Transformer%20Study%20-%20June%202012_0.pdf (accessed March 07, 2022).

6. Bohatyrewicz, P.; Mrozik, A. The Analysis of Power Transformer Population Working in Different Operating Conditions with the Use of Health Index. *Energies* **2021**, *14*, 5213. https://doi.org/10.3390/en14165213

7.   Aslam, M., Haq, I. U., Rehan, M. S., Ali, F., Basit, A., Khan, M. I., & Arbab, M. N. (2021). Health Analysis of Transformer Winding Insulation Through Thermal Monitoring and Fast Fourier Transform (FFT) Power Spectrum. *IEEE Access*, *9*, 114207-114217.

8.   M. Bagheri, M. S. Naderi, T. Blackburn, and T. Phung, "FRA vs. short circuit impedance measurement in detection of mechanical defects within large power Transformer", Conference Record of the IEEE International Symposium on Electrical Insulation (ISEI), pp. 301-305, 2012

9.   Song Wang, Shuang Wang, Ying Cui, Jie Long, Fuqiang Ren, Shengchang Ji, Shuhong Wang, "An Experimental Study of the Sweep Frequency Impedance Method on the Winding Deformation of an Onsite Power Transformer," *Energies*, vol. 13, pp. 3511, 2020.

10.   Cong, Haoxi, et al. "Micro-mechanism study on synergistic degradation of the oil-paper insulation with dibenzyl disulfide, hexadecyl mercaptan and benzothiophene." *High Voltage* (2020).

11.   Charles Sweetser, "Power Transformer Diagnostics: Novel Techniques and their Application", OMICRON, Technical Meeting, 2016

12.   Bagheri, Mehdi, et al. "FRA vs. short circuit impedance measurement in detection of mechanical defects within large power transformer." *2012 IEEE International Symposium on Electrical Insulation*. IEEE, 2012.

13.   Teymouri, Ashkan, and Behrooz Vahidi. "Power transformer cellulosic insulation destruction assessment using a calculated index composed of CO, CO 2, 2-Furfural, and Acetylene." *Cellulose* 28.1 (2021): 489-502.

14.   Georg Brandtzæg, "Health Indexing of Norwegian Power Transformers," Thesis in Engineering of Energy and Environment, Norwegian University of Science and Technology, Master 2015

15.   Ansari, Muhammad A., Daniel Martin, and Tapan Kumar Saha. "Advanced Online Moisture Measurements in Transformer Insulation Using Optical Sensors." *IEEE Transactions on Dielectrics and Electrical Insulation* 27.6 (2020): 1803-1810.

16.   Adusumilli, Pradeep, and SVN Jithin Sundar. "A new criterion for optimal dielectric design of high voltage bushing internal shields in large power transformer." *2019 International Conference on High Voltage Engineering and Technology (ICHVET)*. IEEE, 2019.

17.   Xie, Qiang, et al. "Tests and analyses on failure mechanism of 1100 kV UHV transformer porcelain bushing." *High Voltage Engineering* 43.10 (2017): 3154-3162.

18.   Walczak, Krzysztof, and Jaroslaw Gielniak. "Temperature Distribution in the Insulation System of Condenser-Type HV Bushing—Its Effect on Dielectric Response in the Frequency Domain." *Energies* 14.13 (2021): 4016.

19.   Wang, Dongyang, et al. "Simulation for transient moisture distribution and effects on the electric field in stable condition: 110 kV oil-immersed insulation paper bushing." *IEEE Access* 7 (2019): 162991-163002.

20.   Li, Shijun, et al. "Effect of AC-voltage harmonics on oil impregnated paper in transformer bushings." *IEEE Transactions on Dielectrics and Electrical Insulation* 27.1 (2020): 26-32.

21.   Liu, Jiefeng, et al. "A modified X-model of the oil-impregnated bushing including non-uniform thermal aging of cellulose insulation." *Cellulose* 27.8 (2020): 4525-4538.

22.   Redmil, Redmil presentation on the Slideshare website:http://pt.slideshare.net/rezzmk/redmil-powerpoint, accessed on 20 December 2015

23.   Ndiaye, Ibrahima, et al. *Grid Ready, Flexible Large Power Transformer*. No. Final Technical Report: DE-OE0000852. GE Global Research, 2019.

24.   Dieter Dohnal, "On-Load Tap-Changers for Power Transformers", Maschinenfabrik Reinhausen GmbH Falkensteinstrasse 8 93059 Regensburg, Gemany, 2013

25.   Handley, B., M. Redfern, and S. White. "On load tap-changer conditioned based maintenance." *IEE Proceedings-Generation, Transmission and Distribution* 148.4 (2001): 296-300.

26.   Al-Ameri, Salem Mgammal, et al. "The Effect of Tap Changer Coking and Pitting on Frequency Response Analysis Measurement of Transformer." *2021 IEEE International Conference on the Properties and Applications of Dielectric Materials (ICPADM)*. IEEE, 2021.

27.   Seo, Junhyuck. "Intelligent condition monitoring and diagnosis of a power transformer: on-load tap changer (OLTC) and main winding." (2019).

28. Georg Brandtzæg, "Health Indexing of Norwegian Power Transformers," Thesis in Engineering of Energy and Environment, Norwegian University of Science and Technology, Master 2015

29. Saha, Tapan Kumar, and Prithwiraj Purkait, eds. *Transformer ageing: monitoring and estimation techniques*. John Wiley & Sons, 2017.

30. Brodeur, Samuel, Van Ngan Lê, and Henri Champliaud. "A nonlinear finite-element analysis tool to prevent rupture of power transformer tank." *Sustainability* 13.3 (2021): 1048.

31. Ali Jahromi, Ray Piercy, Stephen Cress, Jim R. R. Service and Wang Fan "An Approach to Power Transformer Asset Management Using Health Index" Kinetrics Inc., Transmission and Distribution Technologies, Toronto, ON, Canada, 2009

32. Wang, Ronglan, Yuying Zhang, and Bo Jiao. "Theory research on high performance control technology of large power transformer strong oil-cooled system." *2020 IEEE 4th Information Technology, Networking, Electronic and Automation Control Conference (ITNEC)*. Vol. 1. IEEE, 2020.

33. Kim, Young Joo, et al. "A numerical study of the effect of a hybrid cooling system on the cooling performance of a large power transformer." *Applied Thermal Engineering* 136 (2018): 275-286.

34. Gao, Xiang, C. Adam Schlosser, and Eric R. Morgan. "Potential impacts of climate warming and increased summer heat stress on the electric grid: a case study for a large power transformer (LPT) in the Northeast United States." *Climatic change* 147.1 (2018): 107-118.

35. Weiping, Ma, et al. "Fault diagnosis on power transformers using non-electric method." *2006 IEEE International Symposium on Industrial Electronics*. Vol. 3. IEEE, 2006.

36. Franzén, Anna, and Sabina Karlsson. "Failure modes and effects analysis of transformers." *Royal Institute of Technology, KTH School of Electrical Engineering, Stockholm, Sweden* (2007).

37. Eyüboğlu, Onur Hakkı, Burak Dindar, and Ömer Gül. "Risk Assessment by Using Failure Modes and Effects Analysis (FMEA) Based on Power Transformer Aging for Maintenance and Replacement Decision." *2020 2nd Global Power, Energy and Communication Conference (GPECOM)*. IEEE, 2020.

38. Ciulavu, Cristina, and Elena Helerea. "Power transformer incipient faults monitoring." *Ann Univ Craiova-Electr Eng Ser* 32 (2008): 72-7.

39. Bustamante, Sergio, et al. "Determination of Transformer Oil Contamination from the OLTC Gases in the Power Transformers of a Distribution System Operator." *Applied Sciences* 10.24 (2020): 8897.

40. Hussain, MD Rashid, Shady S. Refaat, and Haitham Abu-Rub. "Overview and Partial Discharge Analysis of Power Transformers: A Literature Review." *IEEE Access* (2021).

41. IS 10593, "Mineral Oi-impregnated electrical equipment in services - Guide to the interpretation of dissolved and free gases analysis," 2006

42. QI Bo，ZHANG Peng，RONG Zhihai，et al. Differentiated warning rule of power transformer health status based on big data mining［J］. International Journal of Electrical Power & Energy Systems，2020，121：106150.

43. IEEE Standard C57.104-2008: " IEEE Guide for the Interpretation of Gases Generated in Oil-Immersed Transformers," 2008

44. Cheng, L.; Yu, T. Dissolved Gas Analysis Principle-Based Intelligent Approaches to Fault Diagnosis and Decision Making for Large Oil-Immersed Power Transformers: A Survey. Energies 2018, 11, 913. https://doi.org/10.3390/en11040913

45. Cheng, L.; Yu, T.; Wang, G.; Yang, B.; Zhou, L. Hot Spot Temperature and Grey Target Theory-Based Dynamic Modelling for Reliability Assessment of Transformer Oil-Paper Insulation Systems: A Practical Case Study. *Energies* **2018**, *11*, 249. https://doi.org/10.3390/en11010249

46. Haroldo de Faria Jr., João Gabriel SpirCosta, Jose Luis Mejia Olivas " A review of monitoring methods for predictive maintenance of electric power transformers based on dissolved gas analysis, "Renewable and Sustainable Energy Reviews, p. 201–209, 2015

47. Hydroelectric Research and Technical Services Group "Transformer Diagnostics," United States Department of the Interior Bureau of Reclamation, June 2003

48. Serveron Corporation, "DGA Diagnostic Methods," Serveron White Paper, PN 880-0129-00 Rev. B, 2007

49. Ivanka Atanasova-Höhlein, "DGA – Method in the Past and for the Future", Siemens, 2012

50.   Dukarm, James, Zachary Draper, and Tomasz Piotrowski. "Diagnostic Simplexes for Dissolved-Gas Analysis." *Energies* 13.23 (2020): 6459.

51.   Monsef Tahir, "Intelligent Condition Assessment of Power Transformer Based on Data Mining Techniques" Master thesis, University of Waterloo, Ontario, Canada, 2012

52.   K. Pickster, "Determination of Probability of Failure of Power Transformers using Statistical Analysis," Master Thesis, University of the Witwatersrand, Johannesburg, 2015

53.   IEEE Standard C57.106 -2006, "IEEE Guide for Acceptance and Maintenance of Insulating Oil in Equipment," 2006

54.   Sumereder, C. and Muhr, M., "Moisture determination and degradation of solid insulation system of power transformers," Electrical Insulation (ISEI), Conference Record of the 2010 IEEE International Symposium on (pp. 1-4), IEEE, June 2010

55.   Thomas Prevost; "New Techniques for the Monitoring of Transformer Condition," IEEE T&D Conference, Chicago, Illinois, 17 April 2014

56.   E.A. Mohamed, A. Y. Abdelaziz, A. S. Mostafa, "A neural network-based scheme for fault diagnosis of power transformers," Electr Power Syst Res;75(1),29–39,2005

57.   Nisha Barle, Manoj Kumar Jha, M. F. Qureshi, "Artificial Intelligence Based Fault Diagnosis of Power Transformer-A Probabilistic Neural Network and Interval Type-2 Support Vector Machine Approach" International Journal of Innovative Research in Science, Engineering and Technology, Vol. 4, Issue 1, January 2015

58.   M. R. Ahmed, M. A. Geliel and A. Khalil, "Power Transformer Fault Diagnosis using Fuzzy Logic Technique Based on Dissolved Gas Analysis," 21st Mediterranean Conf. Control Automat., pp. 584-589, 2013.

59.   L.M.R. Oliveira, "Desenvolvimento de Métodos de Deteção de Avarias e Algoritmos de Proteção para Aplicação em Sistemas de Monitorização Contínua de Transformadores Trifásicos",Tese de doutoramento, Faculdade de Ciências e Tecnologia da Universidade de Coimbra, 2013.

60.   C. Myers, "Transformer Conditioning Monitoring by Oil Analysis Large or Small; Contaminant or Catastrophe," in proc. First IEE/IMechE International Conference on Power Station Maintenance - Profitability Through Reliability, Edinburgh, UK, 30 Mar.-1 Apr.1998.

61.   Engineering photos, vídeos and articles:http://emadrlc.blogspot.pt/2012/12/chapter-1-power-transformers.html, acedido em 10 de Agosto de 2016

62.   Shayan Tariq Jan, Raheel Afzal, and Akif Zia Khan, "Transformer Failures, Causes & Impact", International Conference Data Mining, Civil and Mechanical Engineering, Indonesia, Feb. 1-2, 2015.

63.   M. Bagheri, M. S. Naderi, T. Blackburn, and T. Phung, "FRA vs. short circuit impedance measurement in detection of mechanical defects within large power Transformer", Conference Record of the IEEE International Symposium on Electrical Insulation (ISEI), pp. 301-305, 2012

64.   R. Singh, A. S. Zadgaonkar, and A. Singh, "Premature Failure of Distribution Transformers - A Case Study," International Journal of Scientific & Engineering Research, vol. 5, n.º 6, pp. 1457-1466, 2014.

65.   Universidade de Coimbra, departamento de física, [Online] disponível em:http://www.fis.uc.pt/data/20072008/apontamentos/apnt_330_15.pdf, acedido em 20 de Dezembro de 2015

66.   Charles Sweetser, "Power Transformer Diagnostics: Novel Techniques and their Application", OMICRON, Technical Meeting, 2016

67.   Technical Brochure No. 227 Guidelines for Life Management Techniques for Power Transformers. CIGRE WG 12.18 Life Management of Transformers, 125 p., 2002

68.   Georg Brandtzæg, "Health Indexing of Norwegian Power Transformers," Thesis in Engineering of Energy and Environment, Norwegian University of Science and Technology, Master 2015

69.   Mário André Soares, " Elementos para a Gestão do Ciclo de Vida de Transformadores Elétricos de Potência", Tese de Mestrado, FEUP, 2011

70.   ABB, (2016), site da ABB http://new.abb.com/products/transformers/transformer-components/ac-bushings-iec/oil-to-air-application/ac-bushings-type-gob, acedido em 20 de Julho de 2016

71. E. A. Feilat, I. A. Metwally, S. Al-Matri, and A. S. Al-Abri, "Analysis of the Root Causes of Transformer Bushing Failures," International Journal of Computer, Electrical, Automation, Control and Information Engineering Vol. 7, nº 6, pp. 791-796, 2013

72. Redmil, apresentação Redmil no site do Slideshare:http://pt.slideshare.net/rezzmk/redmil-powerpoint, acedido em 20 de Dezembro de 2015

73. Dieter Dohnal, "On-Load Tap-Changers for Power Transformers", Maschinenfabrik Reinhausen GmbH Falkensteinstrasse 8 93059 Regensburg, Gemany, 2013

74. MR, site da MR:http://www.reinhausen.com/desktopdefault.aspx/tabid-1551/179_read-335/, acedido em 15 de Junho de 2016

75. A.Franzén and S.Karlsson. "Failure modes and effects analysis of transformers" Technical Report TRITA-EE 2007:040, KTH School of Electrical Engineering, January 2007.

76. World press, site da world press: https://currentpqevent.wordpress.com/, acedido em 20 de Dezembro de 2015

77. Ali Jahromi, Ray Piercy, Stephen Cress, Jim R. R. Service and Wang Fan "An Approach to Power Transformer Asset Management Using Health Index" Kinetrics Inc., Transmission and Distribution Technologies, Toronto, ON, Canada, 2009

78. Pinterest, site: https://pt.pinterest.com/eeportal/power-transformers, acedido em 21 de Dezembro de 2015

79. Cristina Ciulavu, Elena Herrera, "Power Transformer Incipient Faults Monitoring," Transilvania University of Brasov, 2008

80. IS 10593, "Mineral Oi-impregnated electrical equipment in services - Guide to the interpretation of dissolved and free gases analysis," 2006

81. Ena Narang, Er. Shivani Sehgal, Er. Dimpy Singh, "Fault Detection Techniques for Transformer Maintenance Using Dissolved Gas Analysis," IJERT, Vol. 1 Issue 6, 2012

82. IEEE Standard C57.104-2008: " IEEE Guide for the Interpretation of Gases Generated in Oil-Immersed Transformers," 2008

83. Ivanka Atanasova-Höhlein, "DGA – Method in the Past and for the Future", Siemens, 2012

84. Fabio Scatiggio, "Appraisal of Transformers using Gas-Monitoring Systems," Transformer Life Management Conference, Terna, 2013

85. Haroldo de Faria Jr., João Gabriel SpirCosta, Jose Luis Mejia Olivas " A review of monitoring methods for predictive maintenance of electric power transformers based on dissolved gas analysis, "Renewable and Sustainable Energy Reviews, p. 201–209, 2015

86. Hydroelectric Research and Technical Services Group "Transformer Diagnostics," United States Department of the Interior Bureau of Reclamation, June 2003

87. Serveron Corporation, "DGA Diagnostic Methods," Serveron White Paper, PN 880-0129-00 Rev. B, 2007

88. Portal net, site: http://www.portalnet.cl/comunidad/software.479/1173260-busco-programa-triangulo-de-duval-para-aceite.html, acedido em 21 de Dezembro de 2015

89. Monsef Tahir, "Intelligent Condition Assessment of Power Transformer Based on Data Mining Techniques" Master thesis, University of Waterloo, Ontario, Canada, 2012

90. K. Pickster, "Determination of Probability of Failure of Power Transformers using Statistical Analysis," Master Thesis, University of the Witwatersrand, Johannesburg, 2015

91. Siemens, site da Siemens: http://www.energy.siemens.com/mx/en/services/power-transmission/transformer-test-laboratory/breakdown-voltage.htm#content=Description, acedido em 23 de Julho de 2016

92. IEEE Standard C57.106 -2006, "IEEE Guide for Acceptance and Maintenance of Insulating Oil in Equipment," 2006

93. Sumereder, C. and Muhr, M., "Moisture determination and degradation of solid insulation system of power transformers," Electrical Insulation (ISEI), Conference Record of the 2010 IEEE International Symposium on (pp. 1-4), IEEE, June 2010

94. Thomas Prevost; "New Techniques for the Monitoring of Transformer Condition," IEEE T&D Conference, Chicago, Illinois, 17 April 2014

95. A. Jahromi, R. Piercy, S. Cress, W. Fan, "An approach to power transformer asset management using health index," IEEE Electr. Insul. Mag.,2, 20–34, 2009

96. Prof. Tyrone Fernando "Analysis of Testing Methodologies for High Voltage Transformers," CEED Seminar Proceedings, 2013

97. Joung Young, Kyung Park, Byeng Youn, Wook Lee, "Diagnostics of Mechanical Faults in Power Transformers – Vibration Sensor Network under Vibration Uncertainty," European conference of the prognostics and health management society, 2014

98. Mazdoor Sangathan, Jawaharlal Nehru, "Power Transformers, Part 7: Loading Guide for Oil-Immersed Power Transformers", IS Standard 2026-7, 2009

99. Matz Ohlen, "Estimating moisture in Power Transformers – How to estimate and what to do," Megger Sweden AB, Box 724, 182 17 Sweden, Transformer-Life-Management Conference, Megger Sweden

100. CIGRE Technical Brochure No. 349, "Moisture Equilibrium and Moisture Migration Within Transformer Insulation Systems," CIGRE WG A2.30, June 2008

101. Brian Sparling, "Assessing Water Content in solid transformer insulation from dynamic measurement of moisture in oil," SMIEEE, GE Energy, Canada, April 2008

102. Maik Koch, "Reliable moisture determination in power transformers," Doctoral thesis, Stuttgart University, 2008

103. Y. Du, M. Zahn, B. C. Lesieutre, A. V. Mamishev, and S. R. Lindgren, "Moisture equilibrium in transformer paper-oil systems," IEEE Elect.Insul. Mag., vol. 15, no. 1, pp. 11–20, Jan./Feb. 1999.

104. Daniel Martin, Olav Krause, Tapan Saha, "Measuring the Pressboard Water Content of Transformers Using Cellulose Isotherms and the Frequency Components of Water Migration," 2016

105. N. Lelekakis, D. Martin, and J. Wijaya, "Ageing rate of paper insulation used in power transformers Part 2: Oil/paper system with medium and high oxygen concentration," IEEE Trans. Dielectr. Electr. Insul., vol. 19, pp. 2009-2018, 2012.

106. N. Lelekakis, D. Martin, and J. Wijaya, "The effect of acid accumulation in power-transformer oil on the aging rate of paper insulation," IEEE Electr. Insul. Mag., Vol. 30, No3, pp 19-26, 2014.

107. V.V. Sokolov, "Transformer is gassing – What to do" Scientific and Engineering Center ZTZ-Service Company, Ukraine

108. Thomas Prevost, "New Techniques for the Monitoring of Transformer Condition," IEEE T&D Conference, Chicago, Illinois, 17 April 2014

109. Tobias Stirl, Raimund Skrzypek, Stefan Tenbohlen, Rummiya Vilaithong, "On-line Condition Monitoring and Diagnosis for Power Transformers their Bushings, Tap Changer and Insulation System" East China Electric Power, 35, pp.196-206, 2007.

110. P. Picher, S. Riendeau, M. Gauvin, F. Léonard, L. Dupont, J. Goulet, C. Rajotte, "New technologies for monitoring transformer tap-changers and bushings and their integration into a modern IT infrastructure", CIGRE A2-101, Hydro-Québec, Canada, 2012

111. IEEE Std C57.152-2013, "IEEE Guide for Diagnostic Field Testing of Fluid-Filled Power Transformers, Regulators, and Reactors," 2013

112. Fouad Brikci, "Vibro-Acoustic Testing Applied on Tap Changers and Circuit Breakers," paper presented in TechCon Conference, Sydney (Australia), May 2010

113. DTCPM, site da DTCPM: http://www.spmateriais.pt/corrosaoeprotecao/?page_id=24, acedido em 14 de Julho

114. T. Charng and F. Lansing, "Review of Corrosion Causes and Corrosion Control In a Technical Facility," TDA Progress Report, March and April 1982

115. Paulo Casimiro, "Materiais de contacto com água para consumo humano, mecanismos de degradação e contaminação", tese de mestrado, Faculdade de Ciências e Tecnologia, 2010

116. FEUP, Probabilidades e estatística disponível [online] em: ehttp://paginas.fe.up.pt/~imf/aulas_pest/uploads/imf_pest_16.pdf, acedido em 18 de Julho de 2016

117. Haukka, Matti, "The subtle effects of iron-containing metal surfaces on the reductive carbonylation of RuCl 3." Dalton Transactions 26, pp:3212-3220, 2006.

118. B. Pahlavanpour, M. Eklund, and K. Sundkvist, "Revised IEC standard for maintenance of in-service insulating oil," Weidmann ACTI, Sacramento, CA, pp. 1–14, 2004

119. Weather Underground site: https://www.wunderground.com.

120. Reicosky, D. C., "Accuracy of hourly air temperatures calculated from daily minima and maxima." Agricultural and Forest Meteorology 46.3 pp: 193-209, 1989.

121. Time and date site: https://www.timeanddate.com/, acedido em 21 de Julho de 2016